INORGANIC ANTIMONY SPECIATION USING TUNGSTEN COIL ATOM TRAP AND HYDRIDE GENERATION ATOMIC ABSORPTION SPECTROMETRY

A THESIS SUBMITTED TO
THE GRADUATE SCHOOL OF NATURAL AND APPLIED SCIENCES
OF
MIDDLE EAST TECHNICAL UNIVERSITY

BY

PINAR AKAY

IN PARTIAL FULFILLMENT OF THE REQUIREMENTS
FOR
THE DEGREE OF MASTER OF SCIENCE
IN
CHEMISTRY

JANUARY 2010

Approval of the thesis**;**

INORGANIC ANTIMONY SPECIATION USING TUNGSTEN COIL ATOM TRAP AND HYDRIDE GENERATION ATOMIC ABSORPTION SPECTROMETRY

submitted by **PINAR AKAY** in a partial fulfillment of the requirements for the degree of **Master of Science in Chemistry Department, Middle East Technical University** by

Prof. Dr. Canan Özgen
Dean, **Graduate School of Natural and Applied Sciences**

Prof. Dr. İlker Özkan
Head of Department**, Chemistry**

Prof Dr. O. Yavuz Ataman
Supervisor, **Chemistry Department, METU**

Examining Committee Members:

Prof. Dr. R. Sezer Aygün
Chemistry Department, METU

Prof. Dr. O. Yavuz Ataman
Chemistry Department, METU

Prof. Dr. E. Hale Göktürk
Chemistry Department, METU

Prof. Dr. Mürvet Volkan
Chemistry Department, METU

Assoc. Prof. Dr. Nusret Ertaş
Faculty of Pharmacy, Gazi University

Date: 03.02.2010

I hereby declare that all information in this document has been obtained and presented in accordance with academic rules and ethical conduct. I also declare that, as required by these rules and conduct, I have fully cited and referenced all material and results that are not original to this work.

Name, Last name: Pınar Akay

Signature:

ABSTRACT

INORGANIC ANTIMONY SPECIATION USING TUNGSTEN COIL ATOM TRAP AND HYDRIDE GENERATION ATOMIC ABSORPTION SPECTROMETRY

Akay, Pınar M.S.,
Department of Chemistry
Supervisor: Prof. Dr. O. Yavuz Ataman

January 2010, 111 pages

Antimony is a toxic element which is mostly found in two oxidation states (III and V) in environmental, biological and geological samples. Antimony may form various inorganic and organic compounds that exhibit differences in analytical behavior, toxicity and mobility; inorganic compounds of antimony are more toxic than organic forms and toxicity of Sb(III) has been shown to be 10 times higher than that of Sb(V). Therefore selective determination of Sb(III) and Sb(V) is required in environmental and biological samples. Hydride generation atomic absorption spectrometry is a sensitive, fast and economical technique for the determination of antimony at trace level. A possible non-chromatographic method for antimony speciation is hydride generation atomic absorption spectrometry that is based on the relatively slow kinetics of hydride formation from Sb(V).

In this study, continuous flow hydride generation method for the determination of antimony was developed and hydride generation conditions were optimized. Analyte solution was prepared in 0.050 mol/L HCl and 1.2%

(w/v) $NaBH_4$ stabilized in 0.30% (w/v) NaOH was used as a reductant solution.

Inorganic antimony speciation conditions were determined by continuous flow HGAAS system. For the pre-reduction of Sb(V) to Sb(III), 8.0% (w/v) potassium iodide (KI) and 0.10% (w/v) ascorbic acid were used. Further speciation study was also carried out using Ir coated W-coil Atom Trap Hydride Generation Atomic Absorption Spectrometry.

Tungsten coil atom trap was used to enhance the sensitivity. Tungsten coil surface was treated with Ir and totally 250 µg 1000 mg/L Ir stock solution was used for coating of tungsten coil. LOD and LOQ values were calculated as 152 pg/mL and 508 pg/mL according to 120 seconds trapping. 128 and 37 fold enhancement were obtained for 120 seconds collection with respect to W-coil-ETAAS and ETAAS, respectively.

Keywords: Antimony, speciation, *in-situ* trapping, on-line preconcentration, hydride generation, atomic absorption spectrometry

ÖZ

HİDRÜR OLUŞTURMALI VE TUNGSTEN SARMAL İLE ATOM TUZAKLI ATOMİK ABSORPSİYON SPEKTROMETRİYLE ANTİMON TÜRLENDİRMESİ

Akay, Pınar
Yüksek Lisans, Kimya Bölümü
Tez Yöneticisi: Prof. Dr. O. Yavuz Ataman

Ocak 2010, 111 sayfa

Çevre, biyolojik ve jeolojik örneklerde genel olarak iki yükseltgenme basamağı (III ve V) olan antimon toksik bir elementtir. Antimon farklı davranış, toksiklik ve taşınma özelliklerine sahip çeşitli organik ve inorganik bileşikler oluşturmaktadır. İnorganik antimon bileşikleri organik formlarından daha toksiktir ve Sb(III) türleri Sb(V) türlerinden 10 kat daha fazla toksiklik göstermektedir. Bu sebeple, çevre ve biyolojik örneklerinde antimon türlerinin değerlendirilmesi seçici olmalıdır. Hidrür oluşturmalı atomik absorpsiyon spektrometri kolay, duyarlı ve ekonomik bir yöntem olduğu için düşük düzeylerdeki antimon tayininde kullanılmaktadır. Kromatografik olmayan bir olası yöntem olarak hidrür oluşturmalı atomik absorpsiyon spektrometrisi ile antimon türlendirmesi Sb(V) türlerinin indirgen çözeltisiyle verdiği hidrür oluşma reaksiyonun yavaş olması temeline dayanarak gerçekleşmektedir.

Bu çalışmada, antimon tayini için sürekli hidrür oluşturmalı bir yöntem geliştirilmiş ve hidrür oluşturma şartları optimize edilmiştir. Analit çözeltisi

0.050 mol/L HCl içerisinde hazırlanmıştır ve %0.30 (a/v) içerisinde stabilize edilmiş %1.2 (a/v) $NaBH_4$ indirgen çözeltisi olarak kullanılmıştır.

Inorganik antimon türlendirme şartları sürekli hidrür oluşturmalı sistem ile belirlenmiştir. Sb(V) türlerinin Sb(III) türlerine indirgenmesi için %8.0 (a/v) potasyum iyodür ve %0.10 (a/v) askorbik asit kullanılmıştır. Türlendirme çalışmaları iridyum kaplanmış tungsten sarmal atom tuzaklı hidrür oluşturmalı sistem ile uygulanmıştır.

Tungsten sarmal atom tuzağı duyarlılığı artırmak için kullanılmıştır. Tungsten sarmal yüzeyi iridyum ile kaplanmıştır ve kaplama için toplam 250 µg iridyum kullanılmıştır. Gözlenebilme ve tayin sınırları 120 saniye toplama süresine göre sırasıyla 152 ve 508 pg/mL olarak hesaplanmıştır. 120 saniye toplama süresi ile, W-sarmal-ETAAS tekniğine göre 128 kat, ETAAS tekniğine göre 37 kat duyarlılık artışı elde edilmiştir.

Anahtar Kelimeler: Antimon, türlendirme, *in-situ* tuzaklama, önzenginleştirme, hidrür oluşturma, atomik absorpsiyon spektrometri

To My Family

ACKNOWLEDGEMENTS

I wish to express my gratitude to my supervisor Prof. Dr. O. Yavuz Ataman for his guidance, understanding and suggestions throughout this research.

I would like to thank deeply to Yasin Arslan and Dr. Sezgin Bakırdere for their advice, constructive comments and friendship.

I am deeply grateful to Emrah Yıldırım, İlknur Demirtaş and Selin Bora for their help, support and endless friendship. They always support and encourage me and they are always with me whenever I need them. I would like to thank all AtaMAn Research and C-50 group members for their understanding and friendship.

I would like to thank Necati Koç and Hamit Çağlar for their help during my study.

I would like to express my special thanks to Eda Durkan for her friendship and understanding.

Finally, my special thanks to my mother, father, brother and Görkem Mercan for their trust, patience and love. They always provided me continuous understanding and support.

ABBREVIATIONS

AAS	Atomic Absorption Spectrometry
AFS	Atomic Fluorescence Spectrometry
AT	Atom Trapping
CRM	Certified Reference Material
C_0	Characteristic Concentration
CHG	Chemical Hydride Generation
CF	Continuous Flow
E	Enhancement Factor
EC-HGAAS	Electrochemical Hydride Generation Atomic Absorption Spectrometry
EHQTA	Externally Heated Quartz Tube Atomizer
E_t	Enhancement Factor in Unit Time
ETA	Electrothermal Atomization
ETAAS	Electrothermal Atomic Absorption Spectrometry
ETV	Electrothermal Vaporization
E_v	Enhancement Factor in Unit Volume

FAAS	Flame Atomic Absorption Spectrometry
FITA	Flame in Tube Atomizer
GFAAS	Graphite Furnace Atomic Absorption Spectrometry
GLS	Gas Liquid Separator
GTA	Graphite Tube Atomizer
HCL	Hollow Cathode Lamp
HG	Hydride Generation
HGAAS	Hydride Generation Atomic Absorption Spectrometry
HG-AT-ETAAS	Hydride Generation Atom Trap Electrothermal Atomic Absorption Spectrometry
HG-W-coil-ETV	Hydride Generation Tungsten Coil Electrothermal Vaporizer
ICP-MS	Inductively Coupled Plasma Mass Spectrometry
ICP-OES	Inductively Coupled Plasma Optical Emission Spectrometry
id	Inner Diameter
LOD	Limit of Detection
LOQ	Limit of Quantification
MMQTA	Multiple Microflame Quartz Tube Atomizer
od	Outer Diameter
PTFE	Polytetrafluoroethylene

QTA	Quartz Tube Atomizer
RSD	Relative Standard Deviation
W-coil-AT-HGAAS	Tungsten Coil Atom Trap Hydride Generation Atomic Absorption Spectrometry

TABLE CONTENTS

CHAPTERS

LIST OF TABLES

TABLES

LIST OF FIGURES

FIGURES

CHAPTER 1

INTRODUCTION

A good deal of research on environmental, biological and geochemical issues has been devoted to trace metals such as As, Pb, Cd, Hg, Se and Sb. Essentiality, non-essentiality and toxicity that depend on the concentration and the form of the elements have to be considered because of their association with plant, animal and human health. Elements can form compounds that are toxic even in very low concentrations. Therefore, sensitive and precise techniques are required to determine trace metals at low concentrations. The most common methods used for determination of these metals in environmental and biological samples involve sensitive spectroscopic techniques, such as Inductively Coupled Plasma Optical Emission Spectrometry (ICP-OES) and Inductively Coupled Plasma Mass Spectrometry (ICP-MS). These techniques offer good analytical performance in terms of response, linearity and detection limits. Moreover, preconcentration techniques coupled with Atomic Absorption Spectrometry (AAS) are also alternative and economical techniques to detect low concentrations.

1.1 Antimony

Antimony (Sb) is a naturally occurring element with the atomic number 51 and atomic weight 121.76. Sb can exist in a variety oxidation states (-III, 0, III, V), but it is mainly found as Sb(III) and Sb(V) in environmental, biological and geochemical samples. Sb is geochemically categorized as a chalcophile element and mainly occurs in nature as Sb_2S_3, stibnite, and Sb_2O_3, valentinite.

1.1.1 Occurrence

The rare element Sb has an estimated abundance of 0.2-0.3 mg/kg in the earth crust. Sb is present in the environment as a result of natural processes and anthropogenic activities. Important anthropogenic sources of antimony in soil are vehicle emissions and emissions of smelters. It tends to concentrate on soil and its background concentration is 0.3-8.4 mg/kg.

Typical Sb concentration in unpolluted water systems is less than 1 µg/L. The mean Sb concentration in surface marine waters is 184±45 ng/L. Concentration of Sb range from a few ng/L to a few mg/L depending on location. In natural geothermal water systems Sb concentration are so much higher that range from 500 mg/L up to 10 wt. % **(Filella, Belzile, & Chen, 2002)**.

Sb is present in two oxidation states (III and V) in natural waters depending on the redox status of the aquatic environment. Antimony is found as Sb(V) under oxic conditions. Antimonic acid is represented in different formulations such as $H[Sb(OH)_6]$, $Sb(OH)_5$ and $HSbO_3$. SbO_2^+ species exist in very acidic medium and $[Sb(OH)_6]^-$ are the species present in mildly acidic, neutral and alkaline conditions. Antimony pentoxide, Sb_2O_5, is sparingly soluble in water and produces antimonate anion, SbO_4^{3-}, upon dissolution **(Filella, Belzile, & Chen, 2002)**.

Antimony trioxide, Sb_2O_3, has a low solubility in water. In the pH 2-10 range, the solubility of Sb_2O_3 is independent of pH, thus forming an undissociated substance; antimony hydroxide $Sb(OH)_3$ or SbO(OH), sometimes called meta-antimonious acid ($HSbO_2$). Sb(III) is present as SbO^+ or $Sb(OH)_2^+$ in acidic media and as $Sb(OH)_4^-$ or hydrated SbO_2^- in basic media. The free Sb_3^+ ion is stable in solution only at very high acidities **(Filella, Belzile, & Chen, 2002)**.

Antimony(III) chloride used for standard antimony solutions dissolves in strong HCl solutions. There is no clear evidence for interaction of Sb(V) with chloride.

Sb(III) compounds are soluble in alkaline sulfide solutions. The nature of stibnite or antimonite, Sb_2S_3, that is used in experiments are crystalline or amorphous. It is the important source of metalloid Sb.

The methylated species of antimony are found in environmental and biological samples. They usually account for 10% or less of the total dissolved antimony. The abundance of monomethyl species is higher than dimethyl form **(Andreae, Asmodi, Foster, & Dack, 1981)**. Mono-, di-, tri-methyl and triethyl antimony derivatives mostly occur in sediments from rivers and harbours **(Krupp, Grumping, Furchtbar, & Hirner, 1996)**.

1.1.2 Application

Antimony has been used by human cultures since Early Bronze Age. There are some evidence that Sb compounds were used by alchemists and quacks in medicine, veterinary and cosmetics **(Smichowski, 2008)**. It was investigated that the anthropogenic fluxes of Sb has exceeded natural ones for more than 2000 years **(Filella, Belzile, & Chen, 2002)**.

The world reserves of Sb are principally located in China, Bolivia, Russia, South Africa and Tajikistan. The world mine production by the main producing countries in 2005 is represented in Table 1. China was the top producer of Sb with 84% of world share.

Table 1 World mine production of Sb by country in 2005

Country	**tones**	**% of total**
China	126000	84
South Africa	6000	4.0
Bolivia	5225	3.5
Tajikistan	4073	2.7
Russia	3000	2.0
Total world	150000	100.0

The application and uses of Sb has been expanded around 1990. It was mainly used for making alloys, pigments, paints, pharmaceutical preparations, as opacifying agents for enamels, coloring matter for paper and cloth and for vulcanizing. Its modern uses include catalyst in manufacture of PET (polyethylene terephthalate), component in brake linings as S_3Sb_2, cable covering, ammunition and bearings, flame retardants in adhesives, papers, rubber and textiles **(Smichowski, 2008)**. Sb is used in therapeutic agents against major tropical disease. Pentavalent Sb containing drugs are still used in the treatment of a certain parasitic disease *i.e. leishmaniasis* **(Filella, Belzile, & Chen, 2002)**.

1.1.3 Toxicity and Health Effects

In general, only limited information is available for assessing the impact of antimony on human health. Antimony is a non-essential element for plant, animal and human and its chemical and toxicological properties are similar to arsenic. The toxicological, physiological and chemical properties of antimony depend on its oxidation states, presence of binding partners and potential ligands. Inorganic antimony species are more toxic than organic ones. Elemental antimony is more toxic than its salts and trivalent species of antimony show ten times higher acute toxicity than pentavalent species of antimony. Subchronic toxicity of antimony on different tissues on rats after a 90-day exposure via drinking water was investigated **(Miekeley, Mortari, & Schubach, 2002)**.

The toxicity of ions is determined by measuring median lethal dose (LD_{50}) values. The different LD_{50} values for antimony are given in Table 2 **(Ali & Aboul-Enein, 2006)**.

Table 2 LD_{50} values of some antimony compounds.

Antimony Compounds	Animals	LD_{50} Values (mg/kg)
Sb(III) or Sb(V)	Rat	100
Sb_2O_3	Rat	3250
Sb_2S_3	Rat	1000
Sb_2O_5	Rat	4000
Sb_2S_5	Rat	1599

According to International Agency for Research on Cancer (IARC) antimony trioxide is supposed to be carcinogenic for humans **(International Agency for Research on Cancer (IARC), 1989)**. Antimony and many of its compounds are listed as pollutants of priority interest by the United States Environmental Protection Agency (USEPA) and European Union. The USEPA drinking water standards for maximum contaminant level goal (MCLG) and maximum contaminant level (MCL) are both 6 µg/L **(USEPA Drinking Water Contaminants, 2009)**. The European Union has established a maximum admissible concentration of antimony in drinking water of 5 µg/L **(Council of the European Communities, 1998).**

Antimony enters the body through lung where it is transported to the blood and the other organs. It enters the cell by passive diffusion. It accumulates in vascularized organs and tissues, especially liver and kidneys. It has high affinity towards the blood cells. Sb(III) shows high affinity for erythrocytes and sulfhydryl groups of cell compositions, while erythrocytes are almost impermeable to Sb(V). Therefore, the enrichment of antimony in blood is caused by high affinity of Sb(III) for erythrocytes **(Filella, Belzile, & Lett, 2007)**. Quiroz et al. **(Quiroz, Gregori, Basillo, Pinto, & Lobos, 2009)** found that antimony levels in the blood of port workers are enriched 5 to 10 times in comparison with control groups. They stated that the influence of the traffic emission directly effects the distribution of antimony between plasma and erythrocytes and between erythrocytes membrane and cytoplasm. Antimony leaves the body through urine and faeces over several weeks. Exposure of antimony was observed through urine samples of lead-battery workers. Elevated concentrations of Sb_2O_3 and stibine (SbH_3) were found in urine samples **(Kentner, Leinemann, Schaller, Weltle, & Lehnert, 1995)**.

People who inhale antimony at concentrations of 3 mg/m^3 for eight months to two years develop hearth problems and stomach ulcers. Moreover, people inhaling antimony at concentration of 9 mg/m^3 for more than nine days have lung, eye and skin irritation. Prolonged exposure to antimony can cause eye, skin, lung and stomach irritation in the form of vomit and diarrhea **(Quiroz, Gregori, Basillo, Pinto, & Lobos, 2009)**.

Antimony is not known to cause cancer, birth defects, or affect reproduction in humans. However, it has been reported that antimony can cause lung, liver and kidney cancer as well as cardiac cell death in laboratory animals **(Quiroz, Gregori, Basillo, Pinto, & Lobos, 2009)**.

1.1.4 Determination Techniques

Atomic spectrometric methods based on Flame Atomic Absorption Spectrometry (FAAS), Electrothermal Atomic Absorption Spectrometry (ETAAS), Atomic Fluorescence Spectrometry (AFS) and plasma based techniques, namely Inductively Couple Plasma Optical Emission Spectrometry (ICP-OES) and Inductively Coupled Plasma Mass Spectrometry (ICP-MS) have been extensively used for the determination of antimony in different kind of samples.

Antimony can be determined in air-acetylene flame free of interferences. However, sensitivity of FAAS is not sufficient to determine Sb at very low concentrations. The most sensitive line of Sb is 217.6 nm. High concentrations of lead, copper and iron can cause spectral interferences at this line. Therefore, a slit width of 0.2 nm has to be employed for the determination of Sb at 217.6 nm in order to prevent the substantial effect of spectral interferences at this wavelength **(Welz & Sperling, 1999)**. Alternatively, 231.2 nm line of Sb can be used for determination of higher concentration of Sb. However, the sensitivity is lower by 30-50% at this line **(Dedina & Tsalev, 1995)**.

The introduction of Sb in gas phase into a spectroscopic source offers an advantage of minimizing the problems resulted from matrix interferences and improves the sensitivity of the measurements. When plasma based techniques are used for detection, gaseous sample introduction promotes more efficient atomization, excitation and ionization of the analyte. For this reason trace and ultra-trace levels determination of Sb can be achieved by hydride generation (HG) combined with diversity of atomic and plasma based techniques **(Smichowski, 2008)**.

Graphite Furnace Atomic Absorption Spectrometry (GFAAS) is another technique to determine Sb in different kind of samples. A rapid determination of Sb and As in soil and sediment samples was performed by GFAAS. The limit of detection of antimony in a 100 mg/mL suspension is 0.03 µg/g (Garcia, Merlos, & Cordoba, 1997). The trace and ultra-trace analysis with GFAAS requires preconcentration step. Sb was preconcentrated on activated carbon as antimony(III)-pyrogallol complex; Sb(V) was reduced to Sb(III) and adsorbed antimony on activated carbon was determined by GFAAS and the detection limit was calculated to be 0.005 mg/L **(Kubota, Kawakami, Sagara, Ookubo, & Okutani, 2001)**. Preconcentration can be performed by coupling HG to GFAAS. It is possible to concentrate hydride species on the inner wall of graphite tube.

Plasma based techniques have a number of analytical advantages over flame techniques. High temperature of plasma decreases the interference effects of interelements. Moreover, they offer rapid determination, multielement analysis, determination of low concentration of elements and high dynamic range (10^5-10^6 orders of magnitude). However, sometimes their detection power is inadequate to determine very low concentration of Sb in environmental samples. This case is more severe for ICP-OES. The detection power of ICP-OES can be improved by hydride generation and/or preconcentration step **(Menegario, Smichowsk, Tonello, Polla, Oliveira, & Santelli, 2008)**. A fully automated on-line system, implemented with HG and

ICP-OES was used for the preconcentration and speciation of Sb in human urine. Low expected levels of Sb in urine samples requires improving detection limit. By using online combination of HG with ICP-OES for Sb determination a detection limit of 70 ng/L was reached **(Pacheco, Gil, Martinez, Polla, & Smichowski, 2007)**.

Recently, AFS coupled to HG has received growing attention because it offers determination of Sb at trace and ultra-trace levels due to its high sensitivity, wide dynamic range (4-6 orders of magnitude), simplicity and low instrumental cost. The detection limits obtained for Sb are comparable to those reported for ICP-MS **(Chen, Krachler, & Shotyk, 2003)**.

1.1.5 Inorganic Speciation of Antimony

Selective determination of elements is required because different oxidation states of an element exhibit different behavior in the environment. The knowledge of speciation can help to explain the mobility, bioavailability, storage, and retention of elemental species in different environmental matrices including human body.

It is well known that inorganic Sb species are most toxic ones and toxicity of Sb(III) is ten times higher than that of Sb(V). Hence, determination of inorganic Sb species in environmental, biological samples is of a great importance. Speciation analysis can be performed by hyphenated techniques using chromatographic separation interfaced with atomic spectrometric techniques for the speciation analysis of Sb in different matrices. A possible non-chromatographic technique is hydride generation AAS; antimony speciation is based on the slow kinetics of hydride formation from the pentavalent state. Inorganic Sb(III) species may form hydride while Sb(V) does not when reacting with tetrahydroborate **(Matusiewicz & Krawczyk, 2008)**.

Erdem and Eroğlu **(Erdem & Eroğlu, 2005)** used a microcolumn of chelating resin with –SH functional groups for the selective matrix separation and enrichment of Sb(III) from water samples. Flow injection HGAAS was used for the determination of Sb(III). The resin was selective to Sb(III) at almost all pH and acidity values employed, whereas Sb(V) was not retained at all and could be determined after reduced by L-cystein. The method was applied to bottled drinking waters for Sb determination and it is found that none of the samples contain Sb above allowed level (5.0 µg/L). Limit of detection based on five times preconcentration was 0.06 µg/L.

Due to the difference hydride forming rates of Sb(III) and Sb(V), pre-reduction of Sb(V) to trivalent state before hydride generation is compulsory when the total content has to be determined. Potassium iodide, alone or mixed with ascorbic acid and L-cysteine are frequently used reagents for this purpose. Miravet et al. **(Miravet, López-Sánchez, & Rubio, 2004)** carried out a study of antimony reduction prior to its determination by HG-AFS. The efficiency of L-cysteine, potassium iodide and potassium iodide/ascorbic acid was studied for this purpose. From the results, L-cysteine was found to be most suitable pre-reducing agent.

1.2 Atomic Absorption Spectrometry

Atomic absorption spectrometry is a most widely used spectroanalytical technique for qualitative detection and quantitative determination of elements. Although AAS dates back to the nineteenth century, in 1955, the actual modern form was developed by Alan Walsh, known as the father of modern AAS, in Australia **(Welz & Sperling, 1999)**. The technique can be used to determine the concentrations of over 70 elements in solution.

The main components of an AA spectrometer are: (1) a radiation source that generates the characteristic narrow-line emission of selected analyte atoms; (2) an atomizer that converts the analyte species into gaseous atoms; (3) a wavelength selector that isolates the line of interest from other emitted lines; (4) a detector that measures the intensity of light.

For AAS, the analyte has to be present in atomic vapor state. Therefore, it is necessary to use an atomizer. Both flames and furnaces are used and the appropriate methodologies are known as flame AAS and graphite furnace AAS, respectively.

1. 2.1 Flame Atomic Absorption Spectrometry

In flame AAS; flame is used for the atomization of the analyte. The task of flame is to vaporize and convert entire sample as far as possible into gaseous atoms. Flame has to supply sufficient thermal energy for the atomization of the analyte. Atomization efficiency depends on types of fuel and oxidant as well as fuel to oxidant ratio. The most widely used flame type is air-acetylene flame. For many elements it offers suitable environment and sufficiently high temperature for atomization; however this temperature is not so high therefore ionization interferences are not important **(Broekaert, 2005)**.

The analyte in aqueous phase is introduced to flame via a nebulizer which converts liquid phase into a mist composed of small droplets, called aerosol, by a pressurized gas flow. The sample aerosol is mixed thoroughly with the fuel gas and auxiliary oxidant in spray chamber before leaving the burner slot above which flame is burning. Depending on the burner head, the flame is generally 5 cm to 10 cm long. The radiation passes through the entire length of flame.

Although FAAS is an easy and widely used technique for the determination of several elements, it has some negative aspects that affect the sensitivity. One is the relatively low efficiency of sample introduction system. The nebulization efficiency does not exceed 10%, therefore most of the sample is not transported to the atomizer and there is a great dilution of the sample by flame gases. The second factor limiting the sensitivity is the short residence time of analyte atoms in the optical path; it is in the order of few milliseconds **(Ataman, 2008)**.

1.2.2 Electrothermal Atomic Absorption Spectrometry

Electrothermal AAS is a sensitive and specific technique for the determination of trace elements. In this technique graphite or metallic cup or furnaces that are heated electrically to high temperatures serve as atomizers. The models were originally developed by L’vov and Massman **(Broekaert, 2005)**. The principal of operation is that a small amount of sample (5-100 µL) is introduced through a small opening to the inner surface of a graphite tube which is located on the optical path. The solvent is evaporated and matrix is ashed in the graphite tube. When the tube temperature is increased rapidly the sample is completely atomized.

Graphite cuvettes are mostly used as a sample holder and atomizer in ETAAS systems. The cuvette is flushed with an inert gas such as argon to protect the cuvette from ambient air. Various stages of heating are required to dry the sample, remove the sample matrix by ashing and finally to atomize the analyte. At the drying stage, the graphite tube is heated to the boiling point of solvent to remove any residual solvent from the solvent. After drying step, ashing process is performed for the destruction sample matrix by heating the tube between 350 and 1200 ºC. Finally the temperature of the graphite tube is raised to between 2000 and 3000 ºC for 2-3 s, allowing the atomization of analyte atoms. At this stage internal gas flow is stopped to increase the residence time of analyte atoms in atomization unit. Additional heating cycles can be applied for the removal of any residual material. Prior to the next use the tube is heated to the maximum temperature for few seconds while argon gas is flushed. This operation is called as cleaning step, is required to remove all the species not volatilized during atomization of analyte.

Since the nebulization is eliminated and residence time of the atoms in the graphite tube are longer than FAAS, the sensitivity is usually about 2-3 orders of magnitude higher than that obtained by FAAS. However, the mostly encountered problem in ETAAS is mainly raised from matrix interferences. This arises from small dilution of sample matrix during atomization step. Thus, the ashing process becomes crucial for the removal of constituents without losing any analyte.

1.3 Vapor Generation

The generation of gaseous phase analytes and their introduction to different kind of atomizers provides an effective method for determination of many elements. Several advantages over nebulization of sample are obtained by vapor generation. Sample introduction efficiency is enhanced due to the elimination of nebulization/spray chamber assembly. Analyte is removed from sample matrix and an on-line preconcentration of analyte may be obtained if needed. Detection limits are lower compared to FAAS. Moreover, vapor generation can be used in speciation analysis as coupled with different techniques. There are several vapor generation techniques to convert analytes into their volatile derivatives such as hydrides, chelates, alkyls, carbonyls, oxides or halides before their detection **(Smichowski & Farias, 2000)**.

1.3.1 Hydride Generation

The most widely used vapor generation technique is hydride generation (HG). Hydride generation is the conversion of analyte in an acidified sample to its volatile form by chemical or electrochemical reactions. Released hydrides are transported by a flow of the purge gas to an atomizer. Hydride generation was applied for the first time by Holak in 1969 for the determination of arsenic using AAS **(Holak, 1969)**.

In principle, HG is a sample introduction technique for the determination of volatile hydride forming elements viz., As, Bi, Ge, Pb, Sb, Se, Sn, and Te in AAS and can be coupled to any atomic detector including AFS, ICP-OES and ICP-MS. Among these, hydride generation atomic absorption spectrometry (HGAAS) is the most often used one due its simplicity and low cost.

1.3.1.2 Chemical Hydride Generation

Mostly two different chemical hydride generation methods are used for the production of volatile hydrides. The first one used in earlier stage is metal/acid system. The March reaction used metal/acid system, most often Zn/HCl, to produce nascent hydrogen for analyte reduction to hydride:

$$Zn + 2H^+ \rightarrow Zn^{2+} + 2H \qquad (1.1)$$

$$A^{m+} + (m+n)H \rightarrow AH_n + mH^+ \qquad (1.2)$$

where *m* and *n*, respectively, is valency of the analyte A in the sample solution and in hydride. Other metal/acid reactions used in hydride generation include the mixture of Mg and $TiCl_3$ reacted with HCl and H_2SO_4 to produce arsine, hydrogen selenide, stibine and bismuthine. Aqueous slurry of Al also reacted with HCl and H_2SO_4 to produce arsine, hydrogen selenide and stibine **(Dedina & Tsalev, 1995)**.

The second technique for hydride formation is BH_4^-/acid reaction. The first hypothesis on the mechanism of hydride generation was postulated by Robbins and Caruso in 1979 and is currently known as the "nascent hydrogen" mechanism **(Robbins & Caruso, 1979)**:

$$BH_4^- + H^+ + 3H_2O \rightarrow B(OH)_3 + 8H \quad (1.3)$$

The resulting atomic hydrogen or "nascent hydrogen" which is thought to be formed during the acid hydrolysis of BH_4^- reduces the analyte to hydride according to reaction 1.2.

The second class of mechanism of hydride generation included all kind of hypotheses except the nascent hydrogen hypothesis. This second class has been termed "non-nascent hydrogen" mechanism. D'Ulivo and coworkers has studied to verify the validity of nascent hydrogen mechanism. However, it was demonstrated that Sn, Bi and Sb hydrides can be generated by direct action of borane complexes; without the need of their decomposition. The postulated mechanism of nascent hydrogen has failed to explain the hydride generation in many different experimental conditions, in a pH range 4.3-12.7 **(D'Ulivo, Baiocchi, Pitzalis, Onor, & Zamboni, 2004)**.

Recently, D’Ulivo et al. **(D'Ulivo, Mester, & Sturgeon, 2005)** presented a study in order to gain further understanding of the mechanism of hydride formation by using GC-MS system and deuterated reagents. They investigated that formation of bismuthine and stibine take place by direct transfer of the hydrogen bound to the boron. On the other hand, hydrogen of GeH_4 and SnH_4 are originated from both acid and $NaBH_4$. The same group has investigated the hydrogen exchange characteristics of hydrides. They have found that hydrogen exchange could take place between formed hydrides with aqueous media at different pH values **(D'Ulivo A. , Mester, Meija, & Sturgeon, 2006)**.

1.3.1.2 Electrochemical Hydride Generation

Electrochemical hydride generation (ECHG) is a possible alternative method of chemical hydride generation to analyze some hydride-forming elements recently. Electrochemical hydride generation was firstly introduced by Rigin **(Rigin, 1978)** to reduce As and Sn to the hydrides in alkaline media for detection by atomic absorption and atomic fluorescence.

In electrochemical HG, volatile species are formed in the cathode surface of an electrochemical cell. The generation of hydride species takes place in sequential events: deposition of the analyte on the surface of the cathode, reduction of the analyte and formation of hydrides followed by their desorption. The marked advantage of ECHG over methods based on the chemical reduction is the elimination of sodium tetrahyroborate reagent which is a potential source of contamination. Thus, this method offers lower analyte concentration in blanks and low detection limits. Additionally, influence of the oxidation states of the analyte on the hydride yield can be reduced, depending on the cathode material used **(Menemenlioğlu, Korkmaz, & Ataman, 2007)**.

1.3.2 Hydride Atomization

The final step for the determination of elements employing hydride generation is atomization and detection. Hydride atomization is the conversion of analyte hydride to free atoms with maximum efficiency and has to be optimized with respect to accuracy and signal-to-noise-ratio. If an atomizer is considered to be an ideal atomizer, it has to fulfill the requirements listed below **(Dedina, 2007)**:

1. Analyte has to be converted to free atoms completely.
2. The atomization of interferences has to be prevented therefore the loss of analyte atoms in the observation volume.
3. Long residence time has to be provided for free atoms in the observation volume.
4. Measurement noise has to be minimized.
5. Analyte preconcentration has to be available in atomizer unit.
6. Atomizer has to be robust and should be operated with minimum effort and minimum cost.

It has been noted that real-world atomizers can approach individual criteria and meet these requirements to some extent. The choice of atomizer depends on the analysis to be performed.

The most widely employed atomizers in HGAAS are flameless or flame-in-tube quartz T-tube (QTA) atomizers which can be heated by an air-actylene flame or electrically. Moreover, electrothermal atomizer is frequently used in hydride atomization **(Dedina, 2007).**

1.3.2.1 Flame-in-tube Atomizers

Flame-in-tube atomizers (FITA) employ a capillary centered in the inlet arm of a special T-tube to introduce either oxygen (air) or hydrogen to the atomizer to support an oxygen-hydrogen diffusion microflame that has a temperature of around 2800 ºC. FITA does not require external heating, but carrier gas should contain enough oxygen to support microflame. Flame-in-tube atomizer was first introduced by Siemer and Hageman **(Siemer & Hageman, 1975)**. They used an unheated quartz tube with a small flame burning in the inside entry tube. In this system hydrogen was used as purge gas and a small amount of oxygen was introduced via capillary. A modified design was used by Dedina and Rubeska **(Dedina & Rubeska, 1980)** to investigate the atomization mechanism of selenium hydride. It was found that atomization of selenium hydrides took place in the presence of free radicals generated in the reaction zone of the hydrogen-oxygen flame. The “radical generating” reactions between hydrogen and oxygen are as follows:

$$H + O_2 \leftrightarrow OH + O \qquad (1.4)$$

$$O + H_2 \leftrightarrow OH + H \qquad (1.5)$$

$$OH + H_2 \leftrightarrow H_2O + H \qquad (1.6)$$

Free radicals are formed in the presence of excess hydrogen. Therefore amount of radicals are based on O_2/H_2 ratio. A rapid decrease in concentration of H radicals has been found when increasing the O_2/H_2 ratio above 0.1 and just before reaching 0.5 that is stoichiometric ratio.

The mechanism of hydride atomization takes place via the interaction of hydride species with H radicals. For the atomization of selenium hydride two consecutive reactions proceed:

$$SeH_2 + H \leftrightarrow SeH + H_2 \qquad (1.7)$$

$$SeH + H \leftrightarrow Se + H_2 \qquad (1.8)$$

It can be seen from the reactions the free Se atoms are generated with deprotonation of SeH_2. Since the probability of formation of free analyte atoms depends on the concentration of H radicals, local atomization efficiency increase with the growing number of free radicals in the inlet arm of the T-tube. At the optimum oxygen flow rate, the hydride is completely atomized within the H radical cloud **(Dedina & Tsalev, 1995)**.

1.3.2.2 Conventional Externally Heated Quartz Tube Atomizers

Conventional externally heated quartz tube atomizer (EHQTA) uses either an electrical resistance or air-acetylene flame to heat the optical tube of the atomizer to a temperature between 700 ºC to 1100 ºC. The use of air-acetylene flame to heat the atomizer was first suggested by Thompson and Thomerson **(Thompson & Thomerson, 1974)** and electrically heated atomizer was introduced by Chu et al. **(Chu, Barron, & Baumgarner, 1972)**. The design is very similar to flame-in-tube atomizers; a T-tube with its bar tube aligned in the optical path and the central arm of T serving for delivery of hydrides carried by a flow of gas from a generator. The carrier gas is usually argon. Hydrogen required for the atomization is supplied from decomposition of tetrahydroborate used for hydride generation. Conventional EHQTA does not employ a special tube to introduce oxygen but a certain content of oxygen in gas mixture is required to reach optimum sensitivity. Oxygen demand mainly depends on the atomization temperature; higher the temperature, lower the demand **(Dedina, 2007)**.

The hydride atomization in the EHQTA appears at the hot zone of the atomizer where a cloud of hydrogen radicals, analogous as in FIT atomizers, is formed by the reactions 1.4 to 1.6 between oxygen and hydrogen. Hyride is atomized within the cloud by same reactions as in FIT atomizers. The exact position of the cloud is controlled by the temperature profile within the atomizer, by the purge gas flow rate and composition, and by the atomizer design. In principle, hydride atomization mechanisms are same for conventional EHQTA and FIT atomizers. The main difference is the technique of creating the hydrogen radical cloud **(Dedina & Tsalev, 1995)**.

1.3.2.3 Multiple Microflame Quartz Tube Atomizers

The disadvantage of FIT atomizer is the short residence time of free analyte atoms in the optical path resulting in low sensitivity. Otherwise its performance is excellent due to the permanent interaction of analyte with hydrogen radicals during atomization. In contrast, conventional EHQTA provides long residence time for the analyte atoms in the optical path resulting in the high sensitivity; however its performance is poor due to the reaction of free analyte atoms with other species in the optical tube after leaving the hydrogen cloud which fills a small portion of the atomizer observation volume. In order to overcome the disadvantages of both atomization techniques Dedina and Matousek **(Dedina & Matousek, 2000)** has designed a new atomizer which is called multiple microflame quartz tube atomizer (MMQTA). The main goal is to fill the whole volume of the atomizer optical bar with hydrogen radicals so that analyte atoms interact permanently with H radicals.

The optical tube of atomizer consists of two concentric tubes. The inner tube has multiple tiny orifices over its length. The oxygen containing gas (either air or argon/oxygen mixture) is introduced inside the outer tube, from where it enters to the inner tube through the orifices. At the orifices, oxygen reacts with hydrogen present inside the tube. A microflame producing H radicals is formed at every orifices, that results in filling the whole observation volume with H radicals. Therefore, analyte atoms can be present in the form of free atoms only.

The multiatomizer provides a better performance than conventiaonal EHQTA by means of higher sensitivity and one to two orders of magnitude better resistance against interferences **(Dedina, 2007)**.

1.3.2.4 Electrothermal Atomizers

Graphite furnaces (GF) have been used for hydride atomization since the introduction of hydride generation. There are two approaches to use graphite furnaces: *in-situ* trapping of hydrides in the furnace and on-line atomization **(Dedina & Tsalev, 1995)**. *In-situ* trapping has been exclusively used for hydride atomization in GF. Basically, hydride purged from the generator is trapped in a heated graphite furnace in the 200-600 ºC range and trapped analyte is atomized at temperatures generally over 2000 ºC. The other approach, on-line atomization in graphite furnaces employs the direct introduction of generated hydride to the furnace preheated to the atomization temperature. The generated hydrides are introduced to the internal gas line of commercial furnaces. The advantage of on-line atomization in GF is a several orders of magnitude better tolerance to atomization interferences than in conventional EHQTA. However, sensitivity for on-line atomization is generally lower than for *in-situ* tapping and conventional EHQTA **(Dedina, 2007)**.

1.3.2.5 Tungsten Atomizer

Although the most widely used electrothermal atomizer is the graphite tube, the limitations such as high power supply requirement, difficulties in the determination of carbide forming elements and its high cost led to the development of metal atomizers. Among the metal atomizer tungsten atomizers have got the priority. The physical and chemical properties of metallic tungsten make these devices versatile alternative electrothermal atomizers and vaporizers for analytical atomic spectrometry. Tungsten devices can function in three different modes: (1) an electrothermal atomizer (ETA) on which liquid sample is dried, ashed and atomized; (2) an electrothermal atomizer in which generated hydride is either atomized or trapped and atomized; (3) an electrothermal vaporizer (ETV) which generates sample aerosol from trapped analyte species that is then carried to a separate atomizer.

The tungsten filament was introduced as an ETA by Williams and Piepmeier for the first time in 1972 **(Williams & Piepmeier, 1972)**. Later, in 1986, Berndt and Schaldach proposed an open system operating with tungsten. In their study, they showed that sensitivity achieved by tungsten coil (W-coil) atomizer is similar to the graphite atomizer **(Berndt & Schaldach, 1988)**. Since then, the tungsten coil as an atomizer for ETAAS has been successfully used for determination of several elements.

The main advantage of W-coil atomizer over graphite furnace is that it needs a relatively simple power supply compared to complicated power system used to heat graphite rapidly. In addition to that it has a high heating rate and its temperature reach to 3200 ºC depending on the applied voltage. Besides, it does not require an extra cooling system which is a requirement for GFAAS, the purge gas is enough for cooling. W-coil atomization allows the determination of carbide forming elements. The other advantage of W-coil atomizer is its low cost **(Ribeiro, Arruda, & Cadore, 2002)**. However, W-coil can be easily oxidized in the presence of O_2 and a reducing environment is required. In order to prevent oxidation a mixture of argon and hydrogen gases is purged through W-coil during atomization or vaporization.

1.3.3 Atom Traps

1.3.3.1 Graphite Furnace Trap

The method of trapping hydride species in a graphite atomizer and the subsequent atomization was described by Drasch et al. **(Drasch, Meyer, & Kauert, 1980)**. They used commercial graphite furnace as a trapping medium as well as atomizer. In this method the hydride of a given element is introduced by a carrier gas into a graphite furnace heated at a certain temperature. Analyte adsorbed on the inner surface of the furnace is thermally decomposed and then atomized at about 2000 º C.

Hydride introduction to furnace is one of the parameters that affects the trapping efficiency. It has to be ensured that hydride should be introduced to the furnace with minimum losses. Generated hydride is introduced via the sample port of graphite tube through an interface made of glass or quartz. A PTFE interface can also be used; however the limitation of PTFE interface is its relatively low temperature resistance. The most convenient and exclusively used interface is quartz capillary inserted through the sampling port of the furnace **(Dedina & Tsalev, 1995)**.

One way of improving trapping efficiency is coating graphite surface by platinum group elements or combination of these elements. Sturgeon *et al.* investigated the applicability of Pd, Pt, Rh and Ru for surface treatment and found that Pd had the best performance among the others. However, the Pd treatment is not permanent and has to be added every time before trapping step **(Sturgeon, Willie, Sproule, Robinson, & Berman, 1989)**. In contrast to Pd, Ir can be used as a permanent modifier if the temperature does not exceed 2300 ºC. Using modifiers not also enhance trapping efficiency but also increase appearance temperature in atomization step.

In-situ trapping has recently achieved considerable progress and it is one of the most exclusively employed hydride atomization method. The reasons for this are that it significantly increases sensitivity, eliminates the effect of generation kinetics and of gas flow on the signal shape and reduces the atomization interferences **(Dedina & Tsalev, 1995)**.

1.3.3.2 Quartz Traps

Another promising approach to atom trapping is to collect hydride in a quartz tube which can be integrated with a quartz tube atomizer. The analyte species can be collected on either the inlet arm of the T-tube or crushed quartz particles placed inside the arm of quartz T-tube. Quartz surface is heated externally to the optimized trapping temperature. After collection of analyte on the quartz surface, temperature is increased for revolatilization of trapped species. Generally H_2 gas is introduced to system to transport the revolatilized species to the atomizer. The distance between quartz trap and atomizer is such an important parameter to be optimized that the decay of volatile species can be observed while they are transported to the atomizer. The other analytical parameters that has critical role on the operation of quartz trap are the temperature of the trap for collection and revolatilization, position of the trap and composition of the carrier gas for both collection and revolatilization **(Ataman, 2008)**.

Korkmaz et al. **(Korkmaz, Ertaş, & Ataman, 2002)** trapped PbH_4 in an externally heated quartz trap with subsequent volatilization and atomization in a conventional EHQTA. They achieved an LOD value of 19 ng/L. Moreover, Korkmaz et al. **(Korkmaz, Dedina, & Ataman, 2004)** replace the conventional EHQTA by a multiatomizer and they trapped stibine in an externally heated quartz trap. Quartz trap with multiatomizer resulted in an LOD of 3.9 ng/L.

Kratzer and Dedina **(Kratzer & Dedina, 2008)** modified the inlet arm of the quartz T-tube to serve as a trap for stibine and bismuthine. They employed a capillary for oxygen delivery to burn out hydrogen during the trapping step. At revolitilization step oxygen purge is closed and hydrogen gas is sent simultaneously. The signal of volatilized analyte atomized in the optical tube was recorded and integrated for 15 s. Under optimized conditions preconcentration efficiency was 100% for both of the analytes.

1.3.3.3 Metal Traps

Resistively heated metal trap is alternative for atom trapping. Among the metal traps, W-coil is used exclusively due to its high heating rate and low cost. It can be taken from a commercial visible tungsten filament. W-coil has been used at about the same time as a trap for the determination of Bi **(Cankur, Ertas, & Ataman, 2002)** and Se **(Barbosa, Souza, & Krug, 2002)** by two independent groups.

Operating principle of W-coil is similar to that of quartz atom trap. W-coil is located in the inlet arm of the conventional EHQTA and connected to a power supply. Generated hydrides are trapped on the surface of resistively heated W-coil. After trapping step, the temperature of W-coil is increased by applied voltage and trapped analyte species revolitilized from surface are transported to the atomizer by purge gases.

W-coil surface can be coated with elements having high boiling and melting points. Surface modification of W-coil provide enhancement for trapping efficiency and the interaction between trapped species and tungsten surface. Recently, the use of iridium coated W-coil for *in-situ* trapping of antimony hydride was described by Alp and Ertaş **(Alp & Ertaş, 2008)**. They proposed that when uncoated W-coil was used a trapping surface, sensitivity could not be improved and the signals were broad and irreproducible. When W-coil was coated with iridium, significant increase in antimony signal was observed. Moreover, Barbosa *et al.* **(Barbosa, Souza, & Krug, 2002)** used a Rh coated W-coil for trapping selenium hydride and reported that coating was stable up to 300 measurement. Same W-coil could be used for approximately 2000 measurements over 60 s collection period and an enrichment factor of 200 was obtained.

Kula et al. **(Kula, Arslan, Bakırdere, & Ataman, 2008)** developed an analytical technique where gaseous SeH_2 is transported and trapped on a resistively heated gold-coated W-coil atom trap for *in-situ* preconcentration. The limit of detection of 39 ng/L was obtained and the enhancement factor of 20.1 was achieved when compared to conventional hydride generation AAS system without trap.

Alternative materials have been proposed for on-line trapping and vapor generation systems using metal traps: A molybdenum strip for the determination of As and Se **(Docekal, Güçer, & Selecka, 2004)**, resistively heated platinum for Cd (İsmail, 2000; Yıldıran, 2008), an externally heated Au wire for Se **(Guo & Guo, 2001)** can be mentioned among these studies.

1.4 Interferences

Two classes of interferences are observed in spectroscopy: spectral and nonspectral. Spectral interferences are observed when radiation is absorbed or emitted by species other than free analyte atoms. Nonspectral interferences result from the influence of sample components on the analyte signal.

Spectral interferences in hydride generation AAS is less serious than liquid sampling AAS because concominants are retained in the condensed phase and analyte is separated from the matrix. Spectral interferences are observed in the presence of very high concentration of hydride forming elements in the sample matrix. Changes in gas flow composition or rates from hydride generators may alter the transparency of flame and cause background absorption. Another reason for background absorption at low wavelengths is due to presence of oxygen that led to the structured absorbance by molecular oxygen in this region **(Dedina & Tsalev, 1995)**. Additionally, background absorption takes place in graphite furnaces when hydrogen generated in the reaction reaches to graphite tube together with the hydride. This background absorption increases markedly with increasing atomization temperature **(Welz & Sperling, 1999)**.

Nonspectral interferences are divided into two groups: (1) liquid phase interferences that occurs during hydride formation and its transfer from solution; (2) gaseous phase interferences that are caused by volatile species produced in hydride generator.

Liquid phase interferences take place due to the changes in the rate of hydride release from the liquid phase and decrease in the hydride release efficiency. These kinds of interferences result from species present in the sample solution. Gaseous phase interferences occur during the transport of hydride from sample solution to the atomizer causing delay or loss of hydride. Additionally, interferences in the atomizer either reducing the atomization efficiency or causing delay in the atomizer can be considered as gaseous phase interferences.

1.5 Aim of the Study

In this study, resistively heated W-coil will be used as a trapping surface and an atomization unit. Conditions for generation of hydride are to be optimized by using continuous flow HGAAS. W-coil atom trap for on-line preconcentration of volatile antimony species will be designed. The analyte species trapped on the W-coil and subsequently atomized. The surface of W-coil will be coated by Ir for surface modification. Conditions will be optimized to collect and atomize analyte species on-line.

Inorganic speciation of antimony is the original contribution planned in this study. Conditions will be optimized to reduce Sb(V) to trivalent antimony by continuous flow HGAAS. Some interference studies will also be conducted.

CHAPTER 2

EXPERIMENTAL

2.1 Chemicals and Reagents

All reagents used throughout this study were of analytical grade or higher purity. Preparation of stock solutions and dilutions were made using 18 MΩ·cm deionized water obtained from a Millipore (Molsheim, France) Milli-Q water purification system which was fed by the water produced by Millipore Elix 5 electrodeionization system. A 1000 mg/L Sb(III) stock solution was prepared by dissolving appropriate amount of potassium antimony(III) tartrate ($C_4H_4KO_7Sb$) (Sigma-Aldrich) in deionized water. A 1000 mg/L Sb(V) stock solution was prepared from potassium pyroantimonate, $K_2H_2Sb_2O_7.4H_2O$, (Fisher Scientific Company) dissolved in boiling water. Working standard solutions of Sb(III) and Sb(V) was prepared by necessary dilutions from stock solutions. All solutions were prepared daily. For acidification of working solutions, proanalysis grade HCl was used (Merck, Darmstadt, Germany). In order to prevent high blank values HCl is purified by using a PTFE subboiled acid distillation system (Berghof, Eningen, Germany).

Working solutions were prepared in 0.050 mol/L HCl solution. Prepared solutions are transported and stored in polypropylene boxes. All glassware and plastic boxes used in the study were immersed in 10% (v/v) HNO_3 solution at least 24 hours and rinsed with deionized water before use.

Reductant solutions were prepared daily from powder sodium tetrahydroborate(III) (Merck, Darmstadt, Germany). For the stabilization of $NaBH_4$ solution, NaOH was used (Riedel, Germany).

For pre-reduction of Sb(V) to Sb(III), 8.0% (w/v) KI (Aklar Kimya, Turkey) and 0.10% (w/v) ascorbic acid (Carlo Erba) were used. Reducing agents were prepared daily in deionized water.

The coating of W-coil was achieved by injecting aliquots of Ir from corresponding 1000 mg/L stock solution (Ultrascientific). Injections were made by using an adjustable volume micropipette.

For the interference study, three different solutions of each selected elements were prepared while keeping Sb concentration constant. Interferent element concentrations were 1, 10 and 100 (m/m) times of analyte concentration. The interferent solutions were prepared from 1000 mg/L stock solutions of Ca (Merck), Al (Merck), As (Merck), Pb (High Purity Standards), Se (High Purity Standards), Sn (Merck), Fe (Merck), Co (High Purity Standards), Ni (Plasma Pure), Cu (High Purity Standards), Hg (Ultrascientific), Cd (High Purity Standards).

2.2 Spectrometers

For continuous flow hydride generation (CF-HGAAS) and hydride generation W-coil electrothermal vaporizer (HG-W-coil-ETV) systems ATI UNICAM 929 atomic absorption spectrometer equipped with a deuterium arc background correction system and 5.0 cm burner head was used. Instrument was controlled and data were processed by the help of Solaar software. A Thermo Electron uncoded Sb hollow cathode lamp was used as the radiation source. The instrumental parameters are given in Table 3.

Table 3 Operating conditions of ATI UNICAM 929.

Parameter	CF-HGAAS	HG-W-coil-ETV
Measurement wavelength, nm	217.6	217.6
Spectral bandpass, nm	0.2	0.2
Lamp current, mA	11	11
Flame type	Stoichiometric Air/Acetylene	Stoichiometric Air/Acetylene
Read time, s	10	10
Measurement mode	Continuous	Peak height

W-coil-AT-HGAAS and HG-AT-ETAAS studies were carried out with a Varian AA140 (Victoria, Australia) atomic absorption spectrometer equipped with a deuterium arc background correction system. Instrument was controlled and data were processed by the help of SpectrAA software (version 5.1). Operating conditions of the spectrometer for W-coil-AT-HGAAS system were shown in Table 4.

Table 4 Operating conditions of Varian AA140

Parameter	Value
Measurement wavelength, nm	217.6
Spectral bandpass, nm	0.2
Lamp current, mA	11
Read time, s	4
Measurement mode	Peak height

2.3 Hydride Generation System

Experiments were carried out in continuous flow using Gilson Minipuls 3 (Villers Le Bell, France) 4-channel peristaltic pumps to transport analyte and reductant solutions. Yellow-blue color coded 1.27 mm i.d. Tygon® peristaltic pump tubings were employed for pumping analyte and reductant solutions through the peristaltic pump. In order to remove waste solution gas liquid separator and Gilson Minipuls 3 4-channel peristaltic pump were utilized.

Solutions were transported by the tubings that were made of polytetrafluoroethylene (PTFE) with 0.56 mm i.d. and supplied from Cole Parmer (USA). The reaction and stripping coil were also made from the same PTFE tubing in different lengths. The 3- way connector used for merging of the analyte, reductant and carrier gas streams were all made of PTFE (Cole Parmer).

Carrier gas which was employed for stripping of solutions and transportation of volatile species to the atomizer was high purity Ar gas that was supplied from Habaş (Ankara). When W-coil was used as both trap and atomizer, H_2 gas (Habaş, Ankara) was also introduced to the system. The flow rates of Ar and H_2 were controlled by two separate rotameters (Cole Parmer). The rotameters were calibrated regularly by a soap bubble flow meter.

Gas liquid separator (GLS) that is made of borosilicate glass was used for separation of gaseous analyte species from the liquid phase. The design of cylindrical type of GLS that was used in this study is shown in Figure 1.

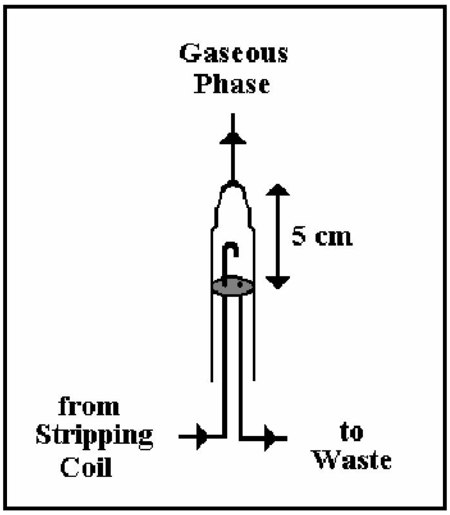

Figure 1 Schematic representation of cylindirical type GLS.

Generated volatile species were transported to the atomizer by PTFE tubing with 0.0635 cm o.d the schematic representation of hydride generation system is given in Figure 2.

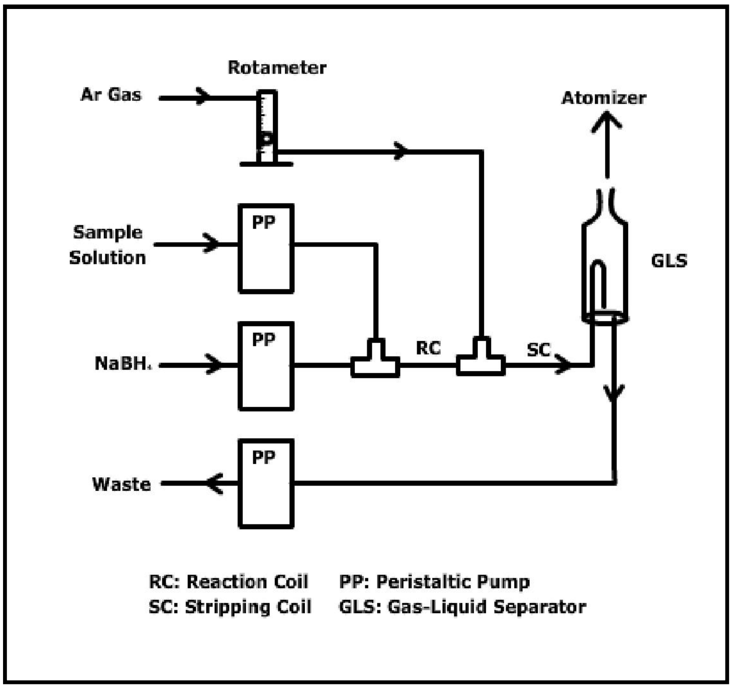

Figure 2 Schematic representation of hydride generation system.

2.4 Atomization Units

2.4.1 Continuous Flow Atomization Unit

A quartz T-tube atomizer was used in hydride generation method. It was heated externally on a stoichiometric air-acetylene flame. The dimensions of quartz T-tube is given in Figure 3. The quartz T-tube atomizers were manufactured by Çalışkan Cam (Ostim, Ankara) and Hazer Cam (Ulus, Ankara). It was placed on a 5.0 cm burner head. At the first use of quartz T-tube, the tube was saturated with 1.0 mg/L Sb(III) solution in order to prevent irreproducible results.

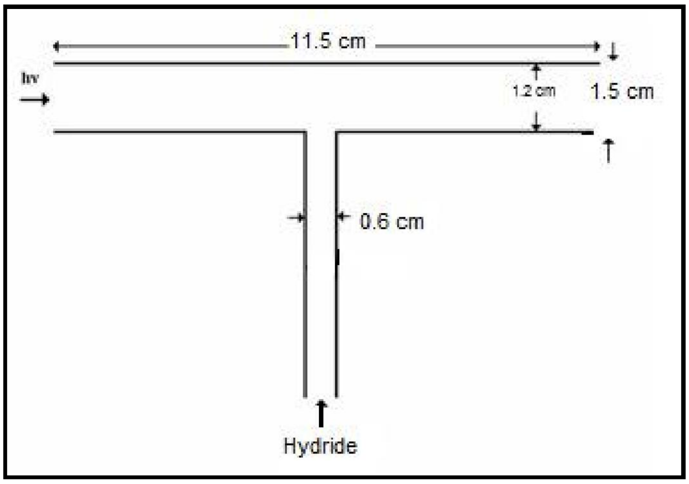

Figure 3 Externally heated quartz T-tube atomizer used in the experiments.

2.4.2 Graphite Furnace Atomization

For *in-situ* trapping of hydride species on graphite furnace trap, outlet of the GLS was connected to the autosampler arm by the help of 0.055 mm i.d PTFE tubing. A quartz capillary with a 0.5 mm i.d. was placed at the tip of the autosampler arm and it was aligned at the injection port of the graphite tube at collection stage. Schematic diagram of the system is given in Figure 4.

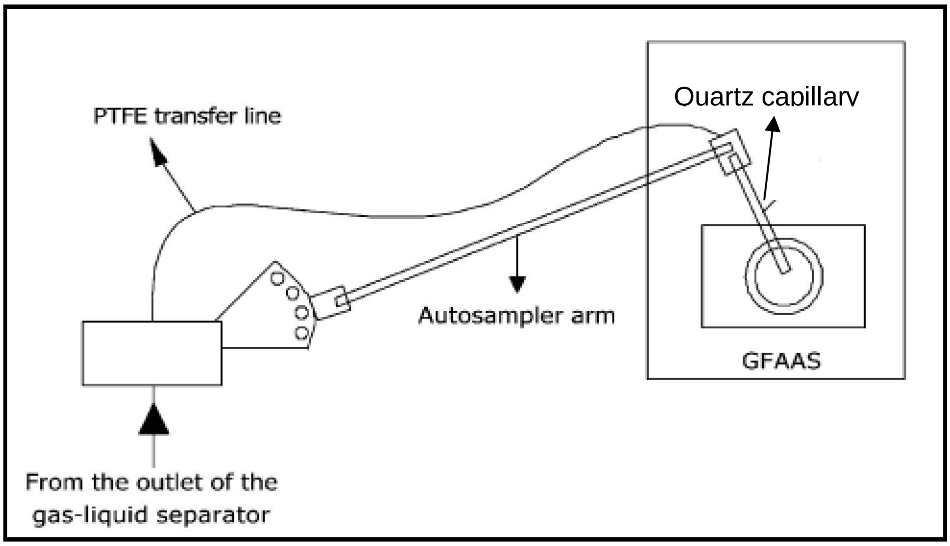

Figure 4 Schematic representation of graphite furnace atom trapping system.

2.4.3 W-coil Atomization Unit

For W-coil-AT-HG system, a W-coil extracted from 150 W, 15 V projector bulb (Philips Focusline, Germany) was used as both trapping and atomization unit. The dimensions of commercially handled W-coils are given in Figure 5.

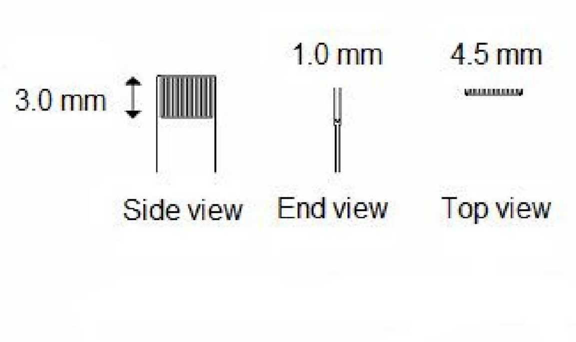

Figure 5 Dimensions of W-coil extracted from a projector bulb.

A glass cell produced in the Glass Shop, Department of Chemistry, METU, was placed on the burner head. W-coil was inserted in the middle of the glass cell from an open hole and fixed with a glass joint which was filled with silicone. Hydride species were introduced to the surface of W-coil through a 0.8 cm o.d. glass tube fixed at the middle of glass cell. Tip of glass tube extended through the glass cell and W-coil was inserted as near as possible to this tip. The side view and schematic diagram of W-coil-AT-HG system are represented in Figure 6 and Figure 7, respectively. The resistive heating of W-coil was achieved by applying an alternative voltage by using a 750 W transformer and a variable potential power supply (Variac) that is connected to main electricity through a power switch. The input voltage of variable potential power supply was 220 V, ac.

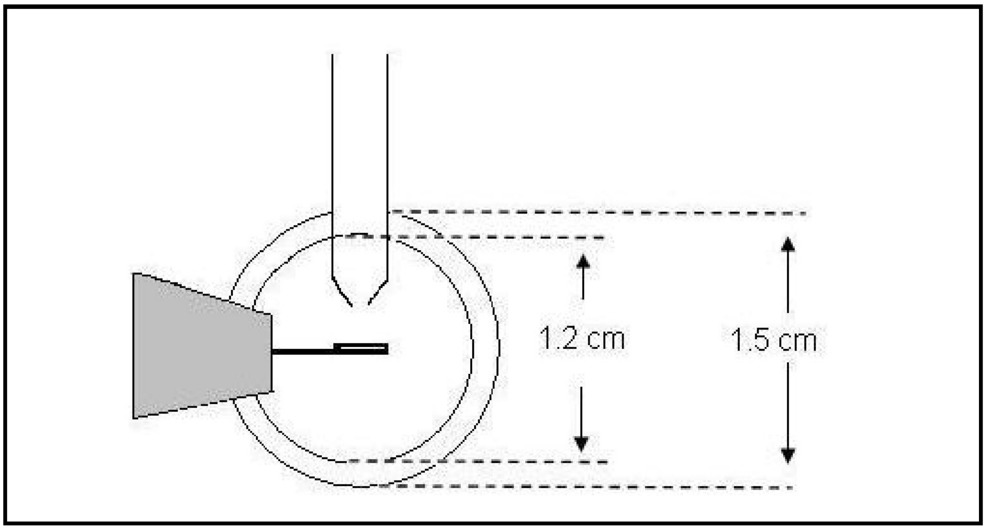

Figure 6 Side view of W-coil-AT-HGAAS system.

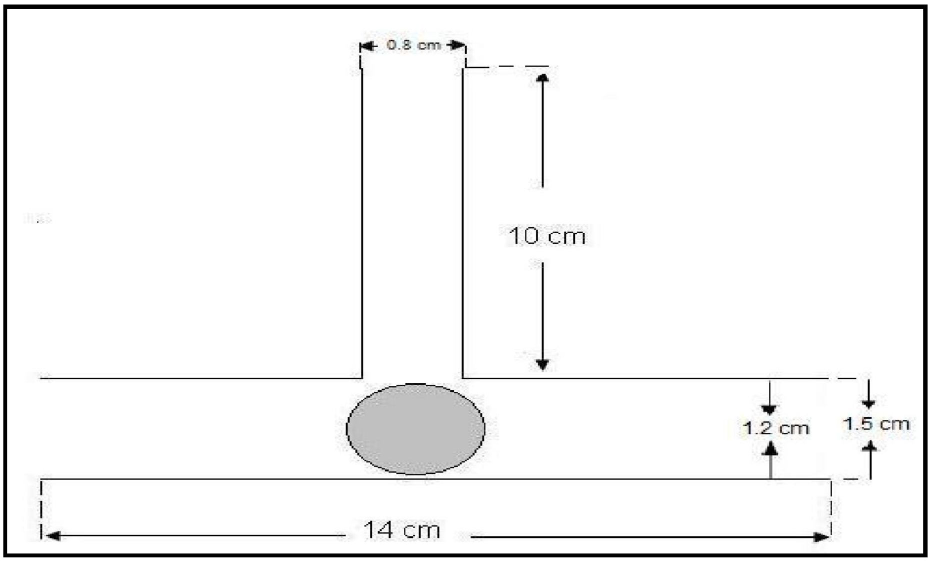

Figure 7 Schematic diagram of W-coil-AT-HG system.

2.5 W-coil as a Vaporizer

In this trap system, W-coil was used as a vaporizer. W-coil was placed in the inlet arm of the conventional EHQTA. It was inserted into the inlet arm of quartz T-tube through an open hole and fixed with a glass joint. Its position was set to supply maximum area for maximum trapping efficiency. Resistive heating of W-coil was same for W-coil atomizer. The schematic diagram of this system is given in Figure 8.

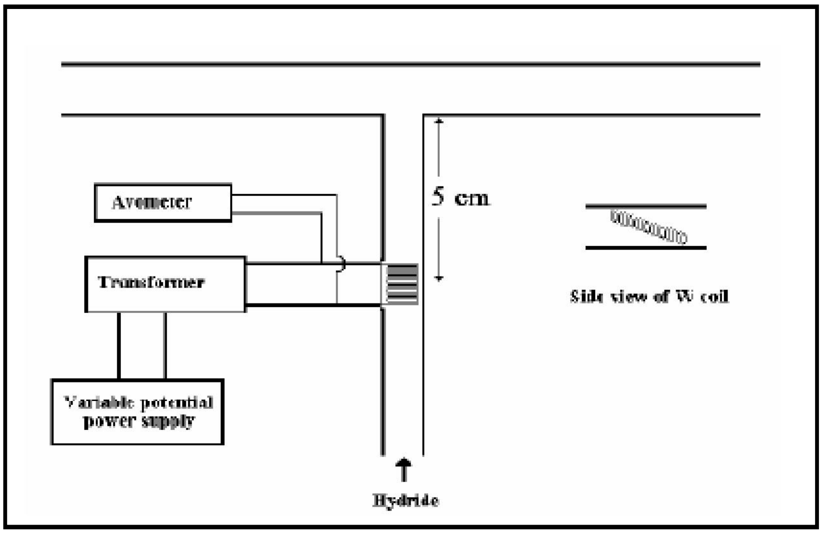

Figure 8 W-coil placed in inlet arm of EHQTA.

Different designs of quartz T-tube for sample introduction were tested. As it is given in Figure 7, volatile species were introduced to W-coil through the inlet arm. Additionally, generated hydrides were sent from top of the W-coil.

When quartz T-tube was used firstly, it was saturated with 1.00 mg/L solution to prevent fluctuations. In these experiments peak height values were recorded.

2.6 Procedures

2.6.1 Continuous Flow Hydride Generation System

In continuous hydride generation system, acidified analyte solution and reductant solution were pumped through peristaltic pumps at a constant flow rate which were 6.0 and 4.4 mL/min, respectively. Argon gas was introduced to the system for stripping of analyte from solution; the optimized flow rate of Ar was 358 mL/min. The duration for one signal at continuous mode was 10 seconds. Each result was the mean of at least two replicate measurements.

2.6.2 W-coil Trapping System

As it was shown in Figure 8, generated hydride species coming from outlet of the GLS was introduced through the inlet arm of the conventional quartz T-tube and trapped on the W-coil heated to a trapping temperature. Peristaltic pumps were active during the collection stage and inactivated when the collection period was over. Temperature of coil was increased rapidly to revolatilization temperature. Released analyte species were transported to the flame heated quartz T-tube atomizer by the help of Ar and H_2 gases. Ar and H_2 gase were introduced from the upstream of the GLS. The function of H_2 gas was to prevent oxidation and promote the release of trapped species from the W-coil surface.

2.6.3 Graphite Trapping System

Outlet of the GLS was connected to autosampler arm as described in section 2.4.2. Temperature program shown in Table 5 was applied for trapping and atomization. Temperature was initiated as the analyte and reductant solutions were pumped through the peristaltic pumps. When the program reached the collection temperature autosampler arm was inserted in the graphite tube and kept inside during collection period. Arm was removed at the end of the collection period and then atomization took place.

Table 5 Temperature program applied for the *in situ* trapping of SbH_3 in graphite tube

Step	Temperature, ºC	Ramp time, s	Hold time, s	Ar flow, L/min
1	85	5.0	5.0	0.30
2	120	5.0	5.0	0.30
3	750	5.0	60.0	0
4*	2000	0.5	1.0	0
5	2000	0.5	2.0	0.30

*Read at this step

2.6.4 W-coil Atomization System

Analyte and reductant solutions were pumped at a constant flow rate by peristaltic pumps as in continuous flow mode. Argon and hydrogen gas were introduced to the system at optimum flow rates. Argon gas was sent upstream of the GLS whereas H_2 was introduced from the downstream of GLS. At collection stage, generated volatile species were transported to W-coil that was heated to collection temperature. After hydride evolution and preconcentration were complete, the pumps were inactivated and W-coil was switched off. All collected analyte species were revolatilized and atomized at once by increasing temperature rapidly to atomization temperature. Ar flow rate was reduced and H_2 flow remained constant during atomization. Since the trap signals were transient and sharp, the peak height values were the basis of the measurements. The integration time was kept 4 seconds. The results obtained throughout the optimization of system were the mean of at least two replicate measurements.

2.6.5 Liquid Sampling Electrothermal Atomic Absorption Spectrometry

Electrothermal atomic absorption studies were performed by the Varian GTA 120 graphite tube atomizer unit. Injection volume of 15 µL was used for standard and sample solutions; Varian PSD 120 programmable sample dispenser was employed. Temperature program given in Table 6 was followed and a transient signal was obtained. Peak height values were the basis of the measurements.

Table 6 Temperature program used for the liquid sampling with ETAAS system.

Step	**Temperature, ºC**	**Ramp time, s**	**Hold time, s**	**Ar flow, L/min**
1	85	5.0	0	0.3
2	95	40.0	0	0.3
3	120	10.0	0	0.3
4	700	5.0	3.0	0
5*	2000	0.7	2.0	0
6	2000	-	2.0	0.3

*Read at this step

2.6.5 Liquid Sampling W-coil Electrothermal Atomic Absorption Spectrometry

Liquid sampling W-coil-ETAAS was performed by using Varian AA140 spectrometer (Victoria, Australia). The glass cell defined in section 2.4.3 was used. W-coil was coated with Ir. Prepared working standard solutions were injected manually onto the W-coil by an adjustable volume micropipette. Injection volume was 20 µL. Temperature program given Table 7 was applied and a transient signal was obtained. Peak height values were taken for this study.

Table 7 Temperature program used for for W-coil-ETAAS.

Step	Time, s	Temperature, ºC	Ar, mL/min	H_2, mL/min
1	45	311	400	136
2	30	470	400	136
3	2	2000	214	136

2.6.6 Coating Procedure

W-coil surface was modified with Ir as a permanent modifier. For coating of W-coil with Ir, 1000 mg/L Ir stock solution was used. 25 µL of Ir solution was injected manually to the surface of W-coil. A temperature program given in Table 8 was then applied. The same procedure was repeated 10 times to increase the coated mass of iridium. During the coating procedure Ar and H_2 flow rates were 400 and 136 mL/min, respectively.

Table 8 Temperature program used for Ir coating.

Step	**Time, s**	**Temperature, ºC**
1	45	311
2	30	470
3	2	1000
4	2	1400

2.6.7 Speciation of Inorganic Antimony Species

Speciation of Sb(III) and Sb(V) was performed by pre-reduction of Sb(V) to Sb(III). Potassium iodide and ascorbic acid were used as reducing agents. The optimum concentrations of these reagents were determined through the continuous flow hydride generation system. The complete reduction of Sb(V) to Sb(III) was achieved with 8.0% (w/v) KI and 0.10% (w/v) ascorbic acid. It was observed that in five minutes Sb(V) was reduced to Sb(III) completely. The speciation studies were carried out solutions containing different ratios of Sb(III) and Sb(V). The procedure optimized in continuous mode was applied with W-coil-AT-HG system.

2.6.7 Accuracy Check

CRM, SCP SCIENCE EnviroMAT Waste Water Low (EU-L-2) was used as a reference material; its content is given in Table 9. Since the certified value was the amount of total Sb, the reduction procedure described in section 2.6.4 was applied.

Table 9 Certified values for SCP SCIENCE EnviroMAT Waste Water, Low (EU-L-2).

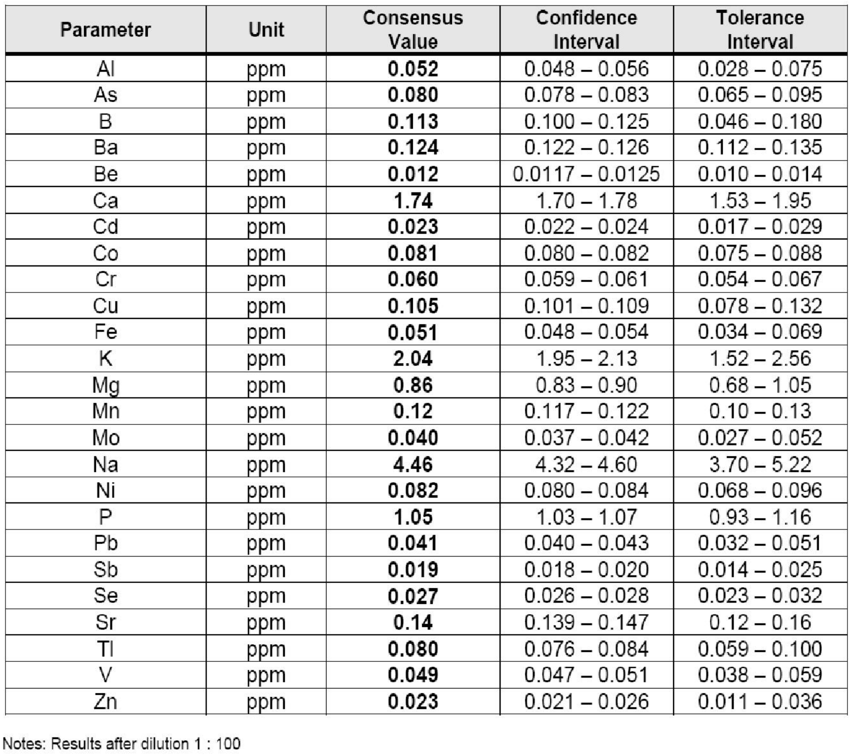

Parameter	Unit	Consensus Value	Confidence Interval	Tolerance Interval
Al	ppm	**0.052**	0.048 – 0.056	0.028 – 0.075
As	ppm	**0.080**	0.078 – 0.083	0.065 – 0.095
B	ppm	**0.113**	0.100 – 0.125	0.046 – 0.180
Ba	ppm	**0.124**	0.122 – 0.126	0.112 – 0.135
Be	ppm	**0.012**	0.0117 – 0.0125	0.010 – 0.014
Ca	ppm	**1.74**	1.70 – 1.78	1.53 – 1.95
Cd	ppm	**0.023**	0.022 – 0.024	0.017 – 0.029
Co	ppm	**0.081**	0.080 – 0.082	0.075 – 0.088
Cr	ppm	**0.060**	0.059 – 0.061	0.054 – 0.067
Cu	ppm	**0.105**	0.101 – 0.109	0.078 – 0.132
Fe	ppm	**0.051**	0.048 – 0.054	0.034 – 0.069
K	ppm	**2.04**	1.95 – 2.13	1.52 – 2.56
Mg	ppm	**0.86**	0.83 – 0.90	0.68 – 1.05
Mn	ppm	**0.12**	0.117 – 0.122	0.10 – 0.13
Mo	ppm	**0.040**	0.037 – 0.042	0.027 – 0.052
Na	ppm	**4.46**	4.32 – 4.60	3.70 – 5.22
Ni	ppm	**0.082**	0.080 – 0.084	0.068 – 0.096
P	ppm	**1.05**	1.03 – 1.07	0.93 – 1.16
Pb	ppm	**0.041**	0.040 – 0.043	0.032 – 0.051
Sb	ppm	**0.019**	0.018 – 0.020	0.014 – 0.025
Se	ppm	**0.027**	0.026 – 0.028	0.023 – 0.032
Sr	ppm	**0.14**	0.139 – 0.147	0.12 – 0.16
Tl	ppm	**0.080**	0.076 – 0.084	0.059 – 0.100
V	ppm	**0.049**	0.047 – 0.051	0.038 – 0.059
Zn	ppm	**0.023**	0.021 – 0.026	0.011 – 0.036

Notes: Results after dilution 1 : 100

CHAPTER 3

RESULTS AND DISCUSSION

This study includes development of an analytical method for speciation of inorganic antimony.

In the first part of the study, continuous flow hydride generation system was performed for the determination of antimony. Optimum conditions for hydride generation of Sb were established. Moreover, speciation studies were carried out with CF-HGAAS system and conditions for complete reduction of Sb(V) to Sb(III) were investigated.

Second part involves the use of W-coil as an atom trap and vaporizer. The conditions of SbH_3 collection, revolatilization stages were tried to be optimized. The results produced with this system were not satisfactory. The reasons were investigated.

Third part includes the trapping of SbH_3 in a heated graphite tube. The main purpose of this study was to investigate whether the problem related to W-coil atom trap was resulted from hydride generation conditions of Sb or not. Satisfactory results were obtained by *in-situ* trapping of SbH_3 on graphite tube. In addition, system performance was evaluated and this method was compared with direct ETAAS determination. HG-AT-ETAAS was used for the calculation of overall efficiency of the HG system.

Fourth part consists of *in-situ* trapping of SbH_3 on W-coil. In this part W-coil was placed into the optical path and employed as an atomizer. Initial studies were carried out with uncoated W-coil, however the results were unsatisfactory. Surface of W-coil was modified with iridium which was used as permanent coating material. The parameters like collection and atomization gas flow rates including Ar and H_2, collection and atomization temperatures and collection period were optimized. Speciation study with W-coil-AT-HGAAS system was performed.

3.1 Continuous Flow Hydride Generation System

This part involves continuous flow hydride generation system and reduction conditions of Sb(V) species. The AAS detection system was used. Flame heated quartz T-tube was used as atomizer.

3.1.1 HCl and $NaBH_4$ Concentrations

Reductant concentration and acidity of analyte are important parameters for the formation of volatile species. In order to find optimum HCl concentration, HCl concentration in the analyte solution was varied between 0.010 to 1.0 mol/L. $NaBH_4$ concentration was ranging between 0.50 to 2.0% (w/v) and all $NaBH_4$ solutions were stabilized in 0.30% (w/v) NaOH. Sample and reductant solutions flow rates were kept at 6.4 and 5.2 mL/min, respectively. Ar flow rate was 615 mL/min and kept constant during the optimization. Variations of analytical signal of 10.0 ng/mL Sb(III) with acid and reductant concentration is given in Figure 9. The increase in the analytical signal up to 0.050 mol/L HCl was observed. The fluctuations in analytical signal for lower acid concentrations were investigated. When the concentration of HCl exceeds 0.050 mol/L the signal decreased. As $NaBH_4$ concentration increases, decrease in signal was observed due to the dilution of analyte species in the excess of H_2 generated. Therefore optimum reductant and acid concentration are 1.2% (w/v) and 0.050 mol/L, respectively.

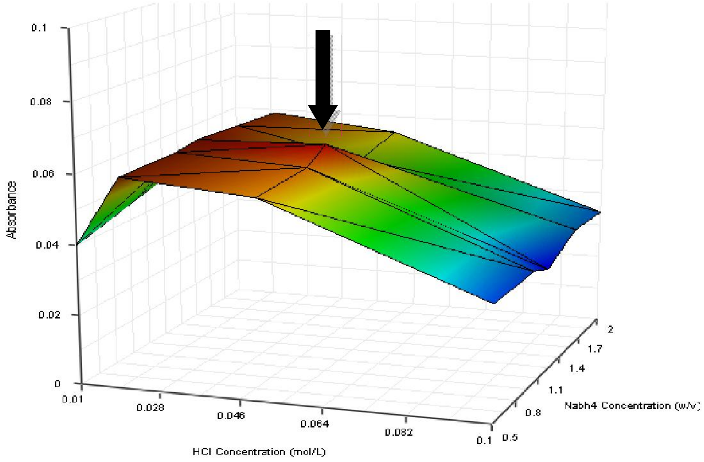

Figure 9 Variation of CF-HGAAS signal with $NaBH_4$ and HCl concentration for 10.0 ng/mL Sb(III) sample solution. Sample and reductant flow rates were adjusted to 6.4 and 5.2 mL/min, respectively.

3.1.2 Sample Solution and $NaBH_4$ Flow Rates

Sample and reductant solutions were merged with different flow rates ranging from 3.0 mL/min to 6.0 mL/min to determine the optimum flow rates. The effect of sample and reductant flow rate is given in Figure 10. As the sample flow rate increases the signal increases. When flow rate of sample is 6.0 mL/min which is selected as optimum value, the intensity of the signal is not changing significantly with the corresponding $NaBH_4$ flow rates.

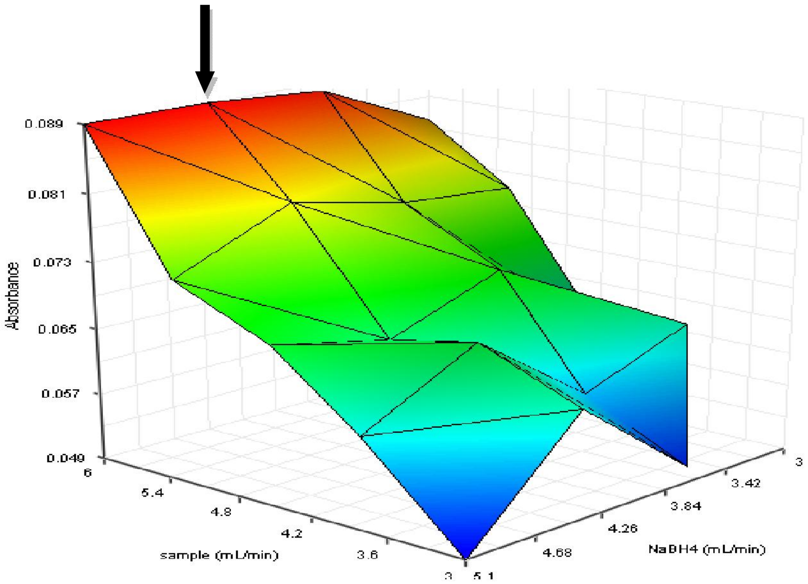

Figure 10 Effect of sample and $NaBH_4$ flow rates on the CF-HGAAS signal of 10.0 ng/mL Sb(III) solution. Sample solution was prepared in 0.050 mol/L HCl and 1.2% (w/v) $NaBH_4$ solutions were used.

3.1.3 Length of Reaction Coil

Reaction coil consists of the tubing between merging point of sample and reductant solutions and the point where argon is introduced as a purge gas (Figure 2). Length of reaction coil is crucial for the complete reaction analyte and reductant. The length was varied between 10 cm to 110 cm. Effect of reaction coil length is given in Figure 11. There was no significant difference in the absorbance values within the lengths. For easy operation 30 cm was selected as an optimum length.

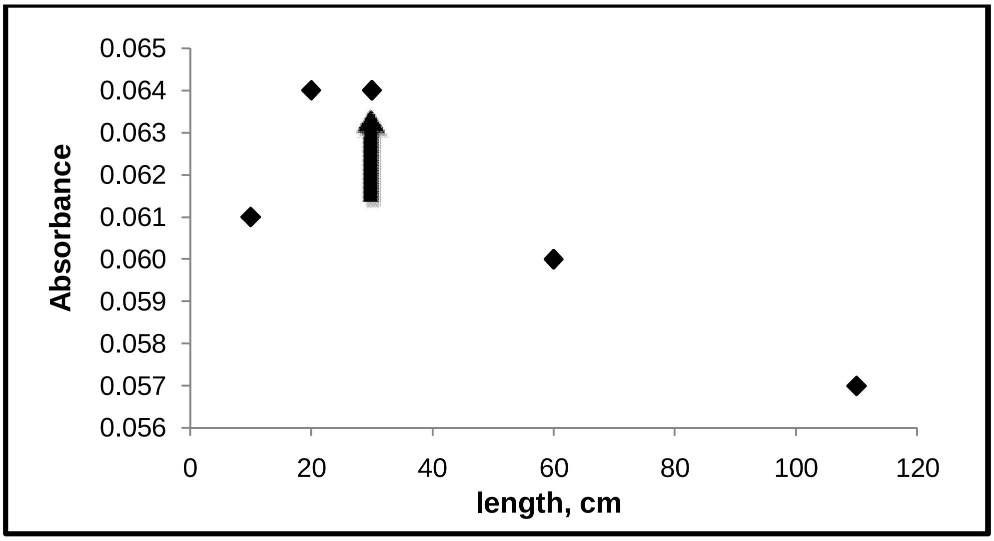

Figure 11 Effect of reaction coil length on analytical signal of 10.0 ng/mL Sb(III). Sample solution was prepared in 0.050 mol/L HCl and has a flow rate of 6.0 mL/min. 1.2% (w/v) $NaBH_4$ was used at 4.4 mL/min.

3.1.4 Length of Stripping Coil

Stripping coil is the tubing between Ar introduction point and GLS (Figure 2). To determine the optimum length of stripping coil, various lengths of PTFE tubings (0.056 mm i.d.) were examined. The effect of stripping coil length on the signal was given in Figure 12. There was not significant variation in the absorbance values with different lengths. For easy operation 25 cm was chosen as an optimum stripping coil length.

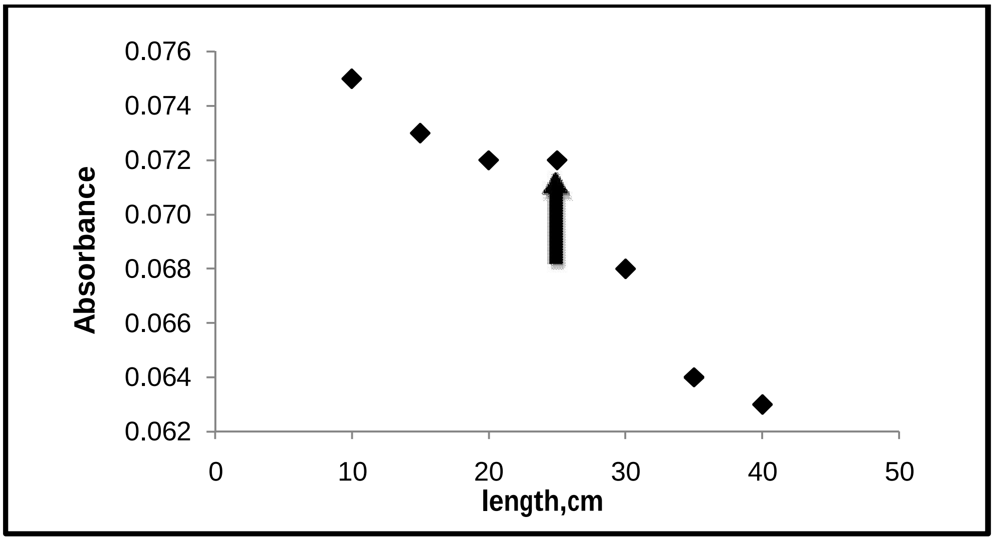

Figure 12 Effect of stripping coil length on analytical signal of 10.0 ng/mL Sb(III). Sample solution was prepared in 0.050 mol/L HCl and has a flow rate of 6.0 mL/min. 1.2% (w/v) $NaBH_4$ was used at 4.4 mL/min.

3.1.5 Stripping Ar Flow Rate

In hydride generation systems different carrier gases are introduced between the reaction and stripping coils to separate the volatile species from the liquid phase and transport these species from GLS to the atomizer. In this study, Ar was used as a carrier gas. The flow rate of Ar gas was important and it affected the analytical signal. Effect of Ar flow rate on the analytical signal is given in Figure 13. Although the absorbance value was higher at low Ar flow rates, signal was not steady during the measurement period. It was clear that low flow rates of Ar were not sufficient to transport volatile species to atomizer in a reproducible and steady manner.

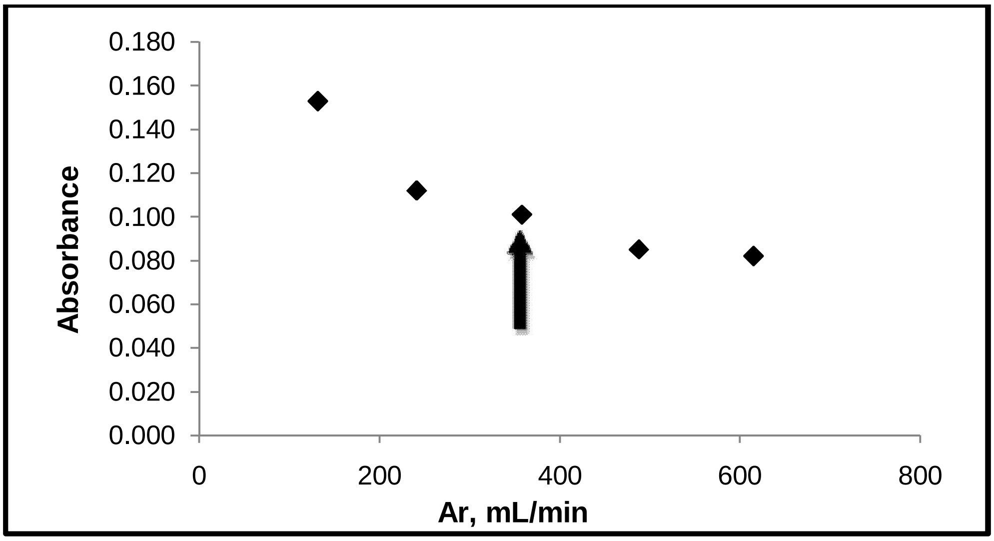

Figure 13 Effect of stripping Ar flow rate on CF-HGAAS signal of 10.0 ng/mL Sb(III) solution. Sample solution was prepared in 0.050 mol/L HCl solution and pumped at 6.0 mL/min flow rate. 1.2% (w/v) $NaBH_4$ was used at a flow rate of 4.4 mL/min.

The optimum flow rate of Ar was selected as 358 mL/min since it gave the most stable signal. At higher flow rates of Ar, analytical signal became smaller due to the dilution of analyte atoms in the EHQTA.

3.1.6 Linear Range and Calibration Plot for Sb(III)

Sb(III) standard solutions between 2-200 ng/mL were prepared to obtain a calibration plot (Figure 14). It was observed that the plot was linear between 2.0 ng/mL to 40.0 ng/mL Sb(III) (Figure 15). After this point deviation from linearity was observed. The best line equation and determination coefficient are $y=0.0069x+0.0023$ and 1.000, respectively.

LOD and LOQ values for the system were 0.55 and 1.84 ng/mL, respectively. LOD and LOQ values were calculated from 7 replicate measurements of smallest concentration of 2.0 ng/mL Sb(III). Characteristic concentration was found as 0.62 ng/mL and calculated from the absorbance value of 20 ng/mL Sb(III). Analytical figures of merit of continuous flow HGAAS is given in Table 10.

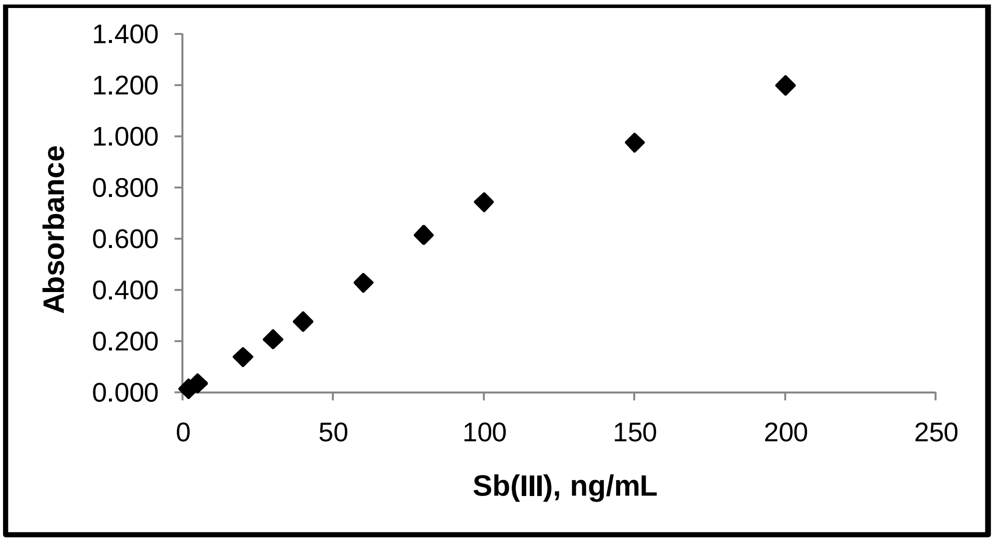

Figure 14 Calibration plot for CF-HGAAS system for Sb(III) solution. Sample solution was prepared in 0.050 mol/L HCl solution and pumped at 6.0 mL/min flow rate. 1.2% (w/v) $NaBH_4$ was used at a flow rate of 4.4 mL/min.

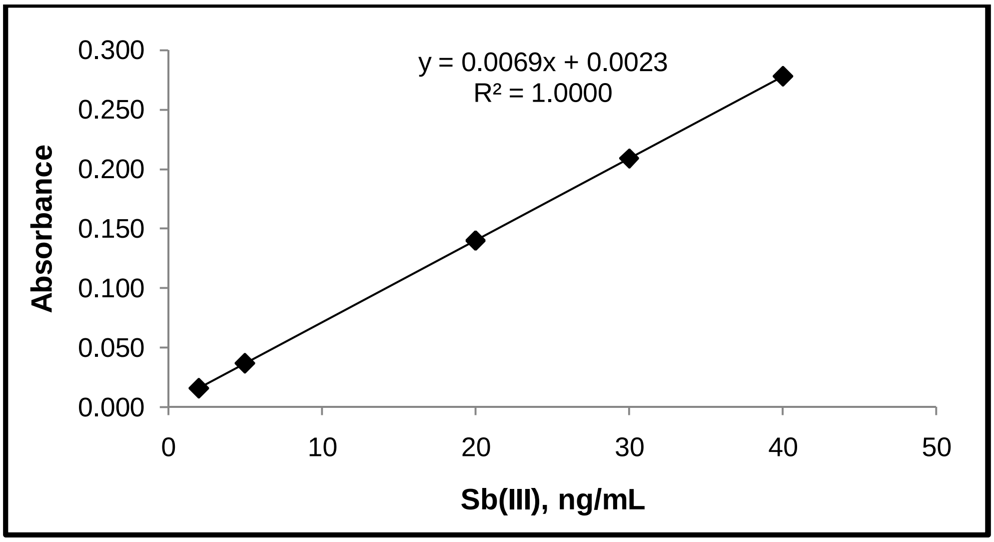

Figure 15 Linear portion of calibration plot for Sb(III) using CF-HGAAS system. Same conditions as in Figure 14 were used.

Table 10 Analytical figures of merit for CF-HGAAS system.

Limit of Detection, LOD, 3s/m (N=7) ng/mL	0.55
Limit of Quantification, LOQ, 10s/m (N=7) ng/mL	1.84
Characteristic Concentration, C_0 ng/mL	0.62

Finally, conditions of CF-HGAAS system were given in Table 11 as a summary.

Table 11 Optimized parameters for CF-HGAAS system.

PARAMETERS	RESULTS
Concentration of HCl, mol/L	0.050
Concentration of $NaBH_4$, % w/v	1.2
Flow rate of sample, mL/min	6.0
Flow rate of $NaBH_4$, mL/min	4.4
Length of reaction coil, cm	30.0
Length of stripping coil, cm	25.0
Carrier gas (Ar), mL/min	358

3.1.7 Speciation Studies

Hydride generation coupled with atomic spectroscopic techniques is widely used for speciation because of its ability in differentiating different oxidation states of hydride forming elements by simple procedures without the use of chromatographic separation **(Kumar & Riyazuddin, 2007)**. It is well known that only trivalent species of Sb form hydride. Since the reaction between pentavalent Sb and tetrahydraborate is very slow, Sb(V) species does not form hydrides. This is the basic principle in inorganic Sb speciation studies. Determination of Sb(III) by HGAAS was performed without any reduction process. For samples containing both trivalent and pentavalent Sb, pre-reduction step was applied to determine the total Sb. The difference between total Sb and Sb(III) gave the concentration Sb(V).

3.1.8 Reduction Process

For the pre-reduction of Sb(V) several reducing agents were applied in the literature. Potassium iodide (KI) alone or mixed with ascorbic acid has been most frequently used for this purpose. In this study KI and ascorbic acid mixture was used as reducing agent. The effect of KI on complete reduction was observed and KI concentration was varied between 1.0 to 10.0% (w/v) and ascorbic acid concentration was kept constant at 0.30% (w/v). 10.0 ng/mL Sb(III) solution was used as a reference to investigate whether Sb(V) was reduced completely or not. There was no complete reduction observed up to 8.0% (w/v) KI. In first ten minutes complete reduction of Sb(V) was achieved with 8.0% (w/v) KI (Figure 16). Optimum KI concentration was selected as 8.0% (w/v).

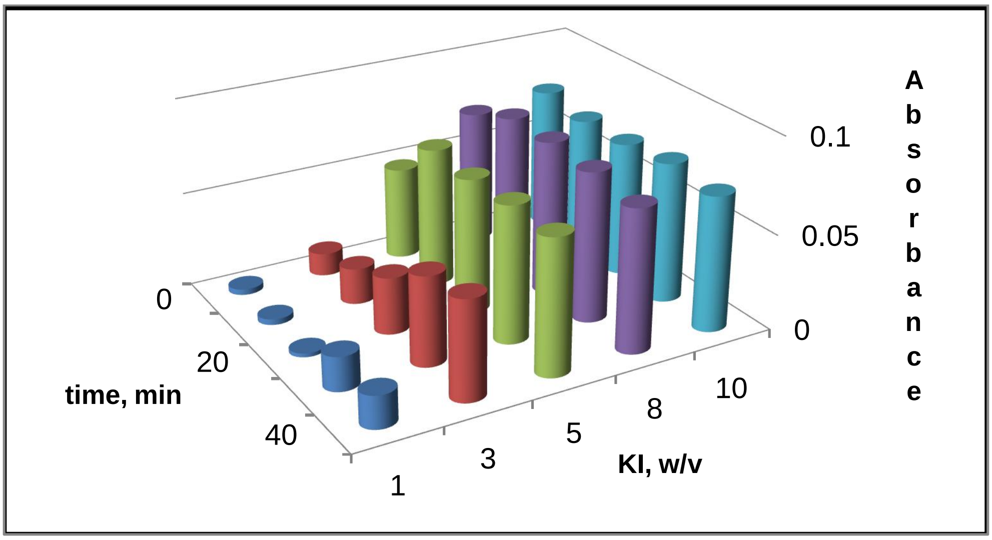

Figure 16 Effect of KI concentration on reduction of 10.0 ng/mL Sb(V) species. Sample solutions were prepared in 0.050 mol/L HCl and 0.30% (w/v) ascorbic acid.

Since KI was not enough for the complete reduction ascorbic acid was used together with KI. To observe the effect of ascorbic acid on the reduction of Sb(V) species concentration of ascorbic acid was varied between 0.0 to 2.0% (w/v) and the KI concentration was kept constant at 8.0% (w/v) (Figure 17). When ascorbic acid was not added to sample solution the reduction rate was very slow and Sb(V) species were not reduced completely. As its concentration increased up to 1.0% (w/v) successful reduction of Sb(V) was obtained. However, as the concentration of ascorbic acid was further increased the analytical signal decreased sharply. 0.10% (w/v) ascorbic acid was selected as optimum value to avoid large amount of reagent consumption.

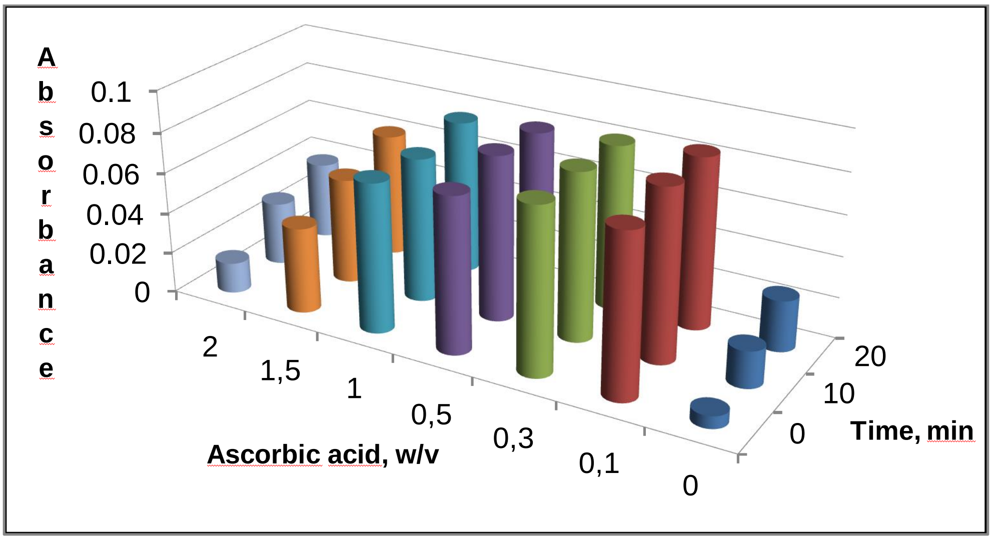

Figure 17 Effect of ascorbic acid concentration on reduction of 10.0 ng/mL Sb(V) species. Concentration of KI was 8.0% (w/v).

After optimizing the parameters of the reduction procedure, sample solutions ranging between 2.0 ng/mL to 40.0 ng/mL Sb(V) were prepared and reduction process for each sample solution was applied. Calibration plot obtained is given in Figure 18.

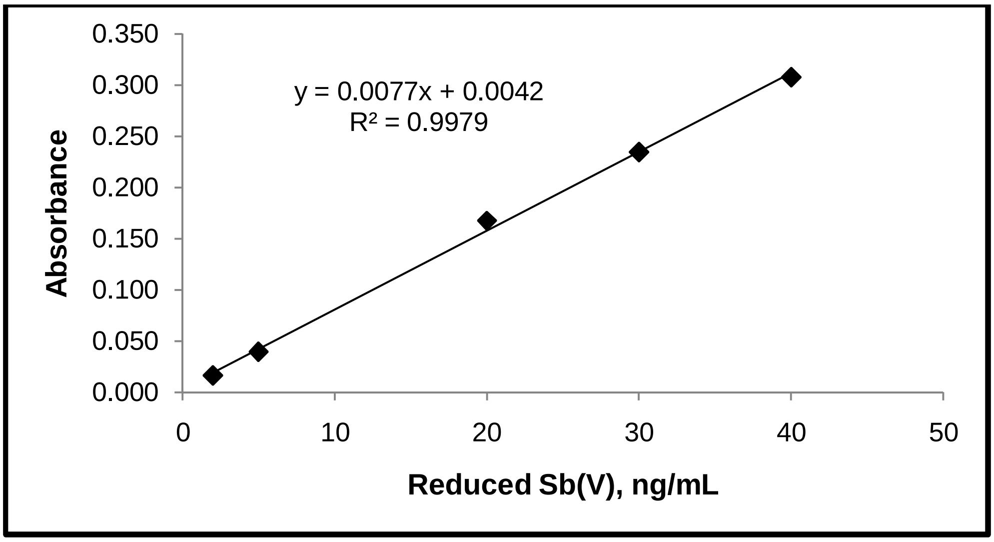

Figure 18 Linear portion of the calibration plot and best line equation for reduced Sb(V) using continuous flow HGAAS.

Analytical parameters for reduced Sb(V) species are given in Table 12. LOD, LOQ and C_0 values were similar to those given for Sb(III). It is clear that reduction of Sb(V) was achieved with very high yield.

Table 12 Analytical figures of merit for reduced Sb(V) species using CF-HGAAS.

Limit of Detection, LOD, 3s/m (N=7) ng/mL	0.59
Limit of Quantification, LOQ, 10s/m (N=7) ng/mL	1.96
Characteristic Concentration, C_0 ng/mL	0.55

Another study was carried out to demonstrate the completeness of reduction for Sb(V) species and show the high yield in reduction. For this study, sets of solutions containing different concentrations of Sb(III) and Sb(V) were prepared as shown in Table13. Total Sb concentration was maintained at 20.0 ng/mL as a final concentration then the reduction procedure was applied.

Table 13 Final Sb(III) and Sb(V) concentrations in mixtures prepared for the reduction system.

Sb(III), ng/mL	Sb(V), ng/mL	Total Sb, ng/mL
0	20.0	20.0
4.0	16.0	20.0
8.0	12.0	20.0
10.0	10.0	20.0
12.0	8.0	20.0
16.0	4.0	20.0
20.0	0	20.0

Prepared mix solutions were reduced with 8.0% (w/v) KI and 0.10% (w/v) ascorbic acid and the plot given in Figure 19 was obtained.

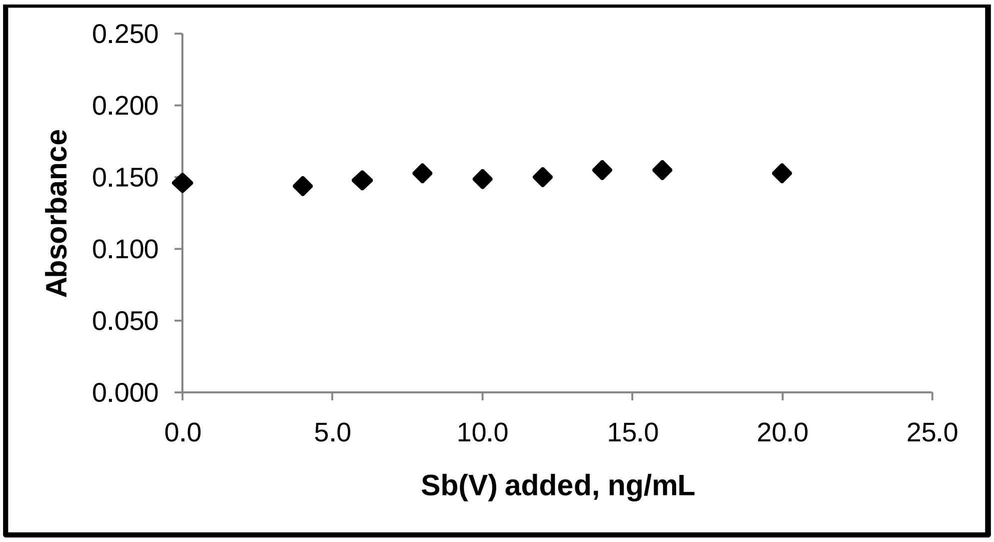

Figure 19 Absorbance values of mixtures after applying prereduction using CF-HGAAS. Total concentration of Sb species was 20.0 ng/mL.

This plot showed that all all Sb(V) species were reduced to Sb(III) by the reduction system optimized. Moreover, prereduction step yielded high recoveries as can be seen from Table 14.

.

Table 14 Recovery values of Sb(V) with CF-HGAAS after prereduction.

Sb(III), ng/mL	Sb(V), ng/mL	Total Sb, ng/mL	% recoveries
20	0	20.0	-
16	4	20.0	98.6
14	6	20.0	101.4
12	8	20.0	104.8
10	10	20.0	102.1
8	12	20.0	102.7
6	14	20.0	106.2
4	16	20.0	106.2
0	20	20.0	104.8

3.2 Hydride Generation W-coil Electrothermal Vaporizer

Continuous flow HGAAS is a technique that allows trace determination of Sb. However, concentration of Sb in samples can be even lower than the LOD of the HGAAS system. In this case hydride generation combined with trapping system can be used to improve the sensitivity. In this part, W-coil was employed as an atom trap and was utilized as a vaporizer.

As it was mentioned in section 2.5 W-coil was located in the inlet arm of EHQTA. Formed hydride species were transported to W-coil that was heated to a certain temperature to collect the hydride species on its surface. This stage was usually called as *collection*. After collection stage, temperature was increased rapidly and trapped species were revolatilized. This stage was named as *revolatilization*. The resultant species were transported to EHQTA for the atomization and transient signal was obtained.

The performance of a fresh W-coil was low at the beginning and it had to be conditioned by applying 10-20 firings to obtain a stable analytical signal. Each coil could be used for 2000 times, but life-time strongly depended on factors causing oxidation.

For the method development several experiments were performed. However some challenges were faced with the system. This will be discussed in the following sections.

3.2.1 Trapped Species on the Quartz Surface

It is well known that quartz is used as trapping medium for the determination of Sb (Korkmaz, Dedina, & Ataman, 2004). W-coil was placed in the inlet arm of the conventional quartz T-tube and it was close to the wall of inlet arm. At the collection stage W-coil was heated to a certain temperature and quartz surface was heated at the same time. Then, during collection stage quartz surface close to W-coil became a trapping medium for stibine. Temperature of W-coil was increased rapidly to revolatilization temperature and kept there for approximately 2 seconds. After atomization, two consecutive signals were observed as given in Figure 20. For this analysis Sb concentration was 10.0 ng/mL. The first peak was the signal for Sb as a result of analyte released from W-coil. The reason for the observation of second peak could be attributed to the release of trapped species from quartz surface with applied revolatilization temperature.

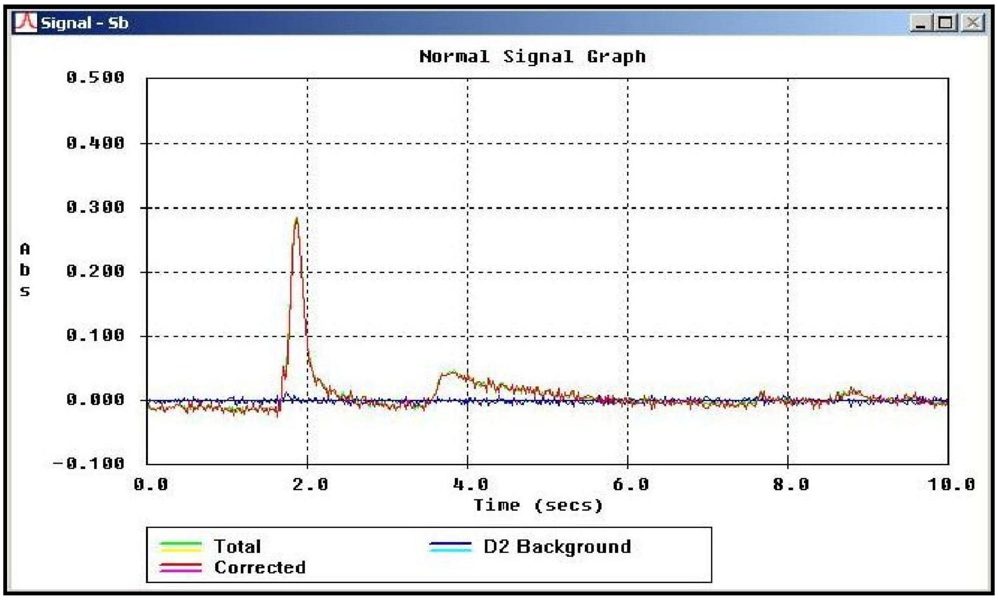

Figure 20 Trapping capability of quartz surface using 10.0 ng/mL Sb when W-coil was used as a trapping medium. Ar flow rate was kept at 135 mL/min for both collection and revolatilizaiton stage and H_2 flow rates at collection and revolatilization stage were 667 and 714 ml/min, respectively.

After each revolatilization cycle, cleaning step was applied under continuous Ar and H_2 gas flow in order to investigate the memory effect. Memory effect was observed after each revolatilization stage. It could be resulted from species remained on W-coil after first revolatilization or revolatilization of trapped species from quartz surface since this part heated up later than W-coil.

3.2.2 Decrease in Analytical Signal

At the revolatilization stage, a high temperature was required to release all trapped species from surface of W-coil. Transport of analyte species to the atomizer was achieved by the help of Ar and H_2 gases. After several firings, a black layer was formed on the quartz surface that was close to W-coil. Signal obtained was not constant and dropped continuously after each firing (Figure 21). It was observed that the absorbance value obtained from last firing was nearly 50% less than that of first firing.

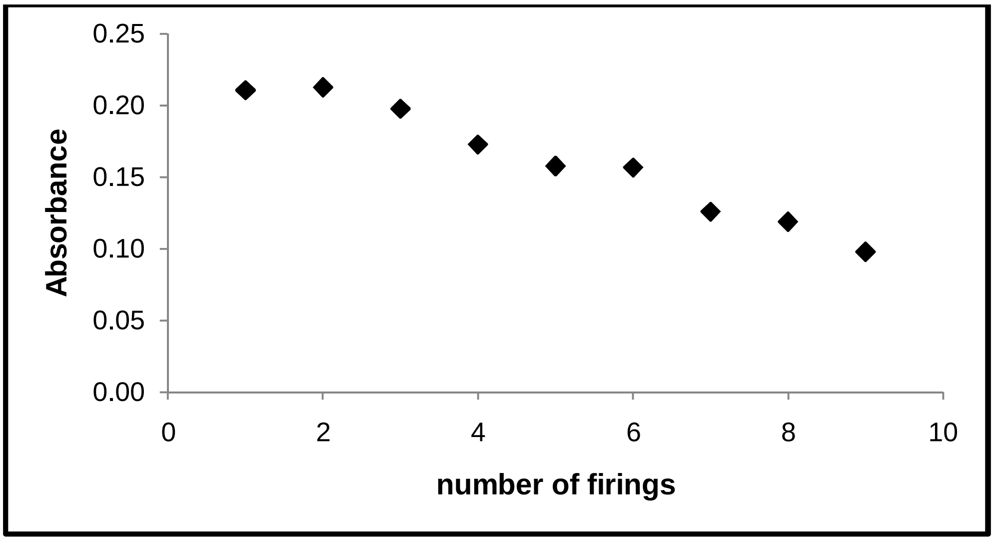

Figure 21 Decrease in analytical signal after formation of black layer on the quartz surface. Concentration of Sb was 10.0 ng/mL.

In order to investigate the nature of black layer formed on the quartz surface, W-coil was used several times and quartz surface close to W-coil was cleaned with a piece of cotton. Black color appeared on the cotton was taken to solution with the help of concentrated HF and this solution was completed to volume of 10 mL with deionized water. Determination of W was performed by ICP-MS after five times dilution from the main solution. Signal of ^{182}W taken from quartz surface is given in Figure 22 demonstrating that black layer contained W. After several firings, tungsten species released from W-coil formed a black layer on quartz surface due to high temperature applied at revolatilization stage.

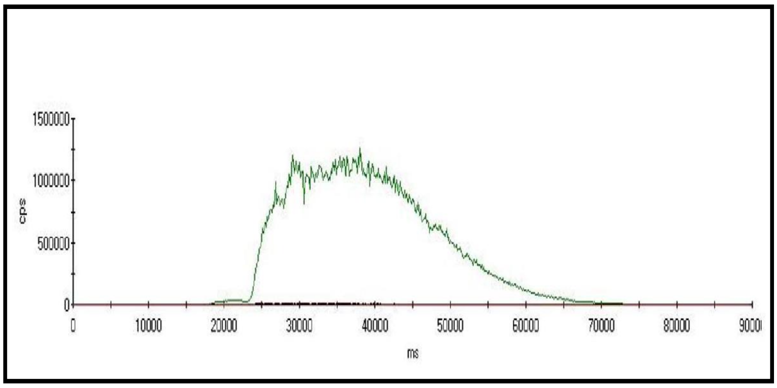

Figure 22 Signal of ^{182}W determined by ICP-MS.

When the black layer was formed, the trapping medium had different characteristic. Then, stibine was trapped on this new surface. The same solution used for W determination was used to determine Sb in the black layer. Determination of Sb was carried out by ICP-MS and signal of ^{121}Sb is given in Figure 23. The signal in blue color was for 10.0 ng/mL Sb and signal in green color was for Sb taken from black layer. It was seen that Sb species were trapped on quartz surface containing W.

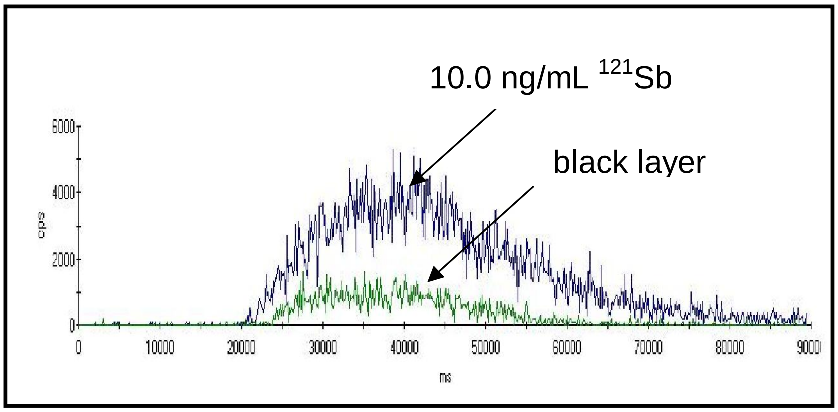

Figure 23 Determination of ^{121}Sb by ICP-MS. Signals in blue color and green color were obtained from 10.0 ng/mL Sb and Sb taken from black layer, respectively.

3.3 *In situ* Trapping of SbH_3 on Graphite Tube

Trapping system of graphite tube was based on the transportation of the generated hydride to a graphite tube heated to an optimized trapping temperature and collecting of hydride species on the graphite surface for an optimized period of time. After collection stage temperature was raised rapidly to the atomization temperature and a transient signal was obtained. No permanent or temporary modifiers were used for surface modification.

The parameters that were optimized in CF-HGAAS were used directly except that the flow rate of stripping Ar. Collection temperature was optimized and linear calibration plot was obtained.

3.3.1 Stripping Ar Flow Rate

For the trapping stage stripping Ar flow rate is important by means of transportation and interaction analyte species with trapping surface. As the Ar flow rate increases transport of analyte is achieved efficiently, but dilution of analyte species in the atomizer occurs. As the flow rate decreases residence time increases; hence the trapping efficiency is enhanced as analyte atoms stay more time in the trapping zone. As a result, stripping Ar flow rate has to be high enough to transport volatile species to atomizer and be as low as possible to increase the residence time. 100 mL/min Ar was selected as an optimum value as indicated in Figure 24. Lower values could not be tested since a reproducible control and measurement could not be made.

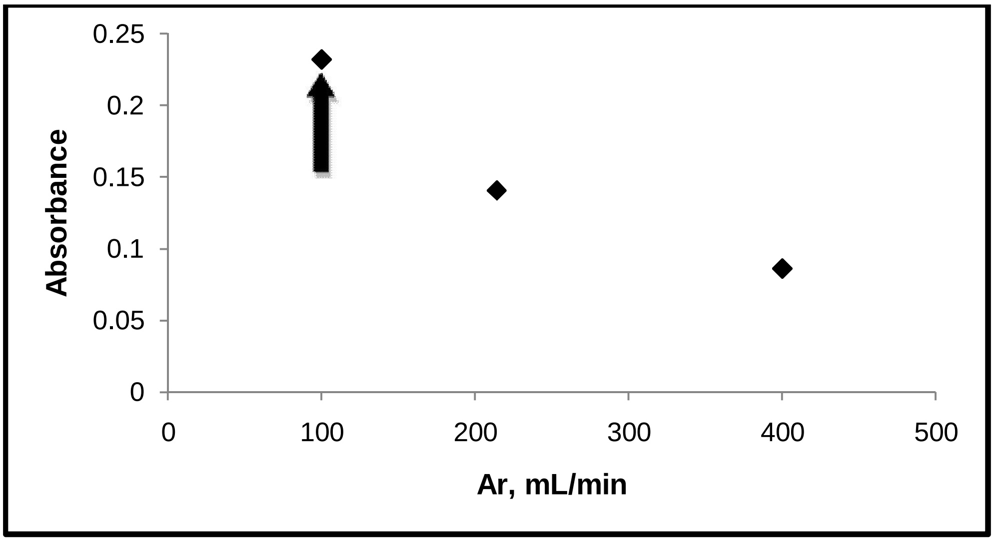

Figure 24 Effect of Ar flow rate on HG-AT-ETAAS signal of 10.0 ng/mL Sb(III) solution trapped over 60 seconds. Sample flow rate was 4.0 mL/min.

As it is expected stripping Ar flow rate in HG-AT-ETAAS, 100 mL/min was lower than that of CF-HGAAS that was 358 mL/min. Low flow rates of Ar resulted in irregular signal in CF-HGAAS (3.1.5) whereas it was possible to work at low flow rates in HG-AT-ETAAS and reproducibility was not a problem.

3.3.2 Collection Temperature

Collection temperature was varied between 200 ºC to 850 ºC while atomization temperature was kept constant at 2000 ºC. Sample and $NaBH_4$ flow rates were adjusted to 4.0 mL/min. Results are shown in Figure 25.

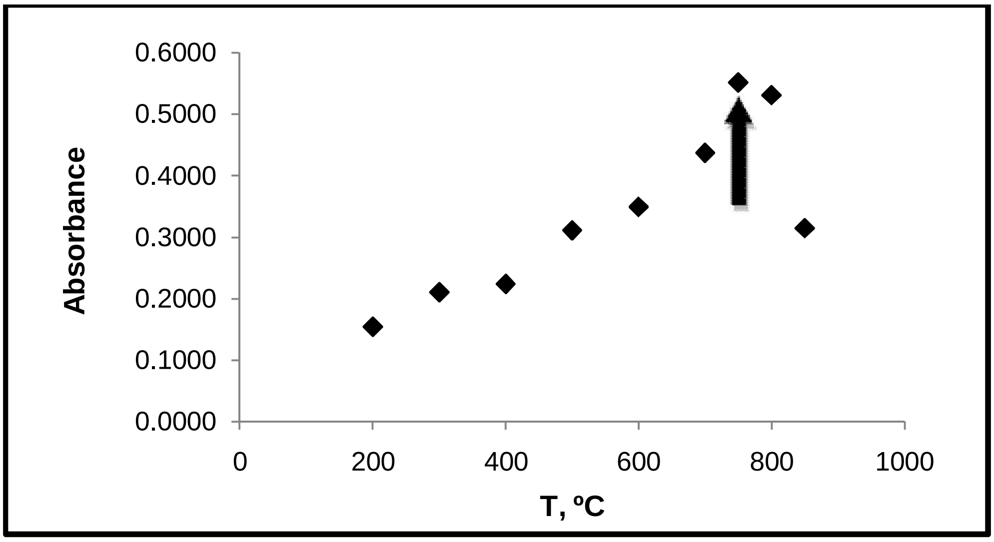

Figure 25 Effect of collection temperature on HG-AT-ETAAS signal of 10.0 ng/mL Sb(III) solution trapped over 60 second time period. Atomization temperature was kept at 2000 ºC. Sample flow rate was 4.0 mL/min.

The optimum collection temperature for SbH_3 reaches a maximum at 750 ºC. At higher temperatures a sharp decrease was observed in the trapping efficiency due to loss of analyte during trapping stage.

3.3.3 Calibration Plot and Linear Range

The calibration plot obtained by peak height for solutions ranging from 0.2 ng/mL to 10.0 ng/mL Sb(III) is given in Figure 26. It was found that the plot was linear between the concentrations of 0.2 ng/mL to 2.0 ng/mL. above this concentration slight deviation from linearity was observed.

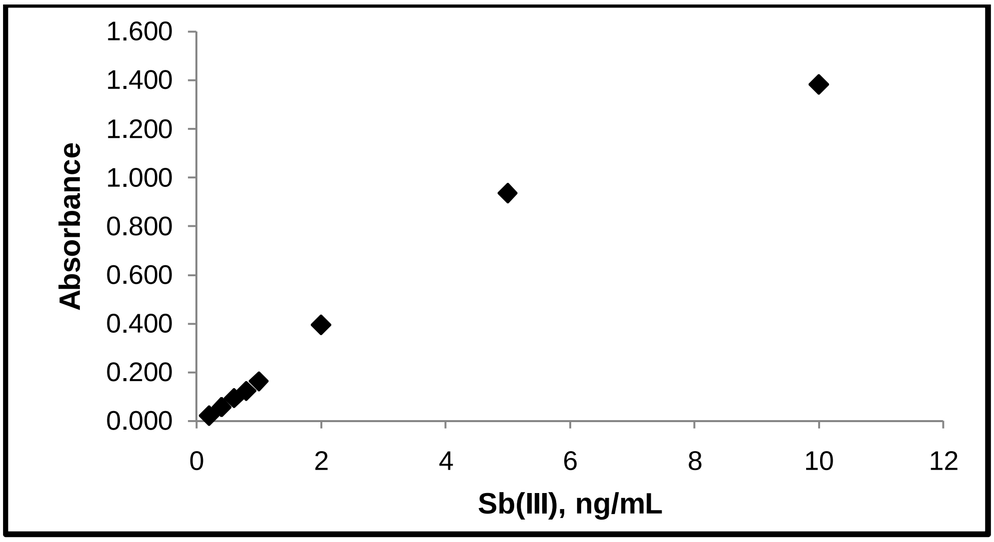

Figure 26 Calibration plot for trapping of SbH_3 on graphite tube using HG-AT-ETAAS. Collection and atomization temperatures were set to 750 and 2000 ºC, respectively. Sample flow rate was 4.0 mL/min. Collection period was 60 s.

A calibration plot and best line equation for HG-AT-ETAAS is given in Figure 27.

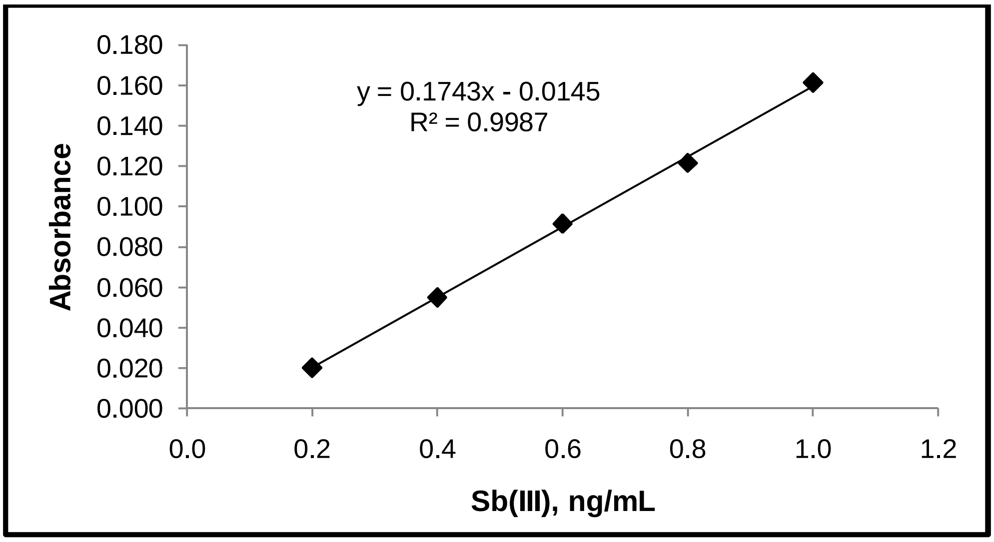

Figure 27 Linear portion of the calibration plot and best line equation for Sb determination by HG-AT-ETAAS using graphite tube. Same conditions as in Figure 26.

3.3.4 Analytical Figures of Merit

LOD and LOQ values were found as 61 pg/mL and 204 pg/mL, respectively and calculated from five replicate measurements of the smallest concentration in the range, 0.2 ng/mL. Characteristic concentration, C_0, was obtained from absorbance value of a 0.6 ng/mL solution and was calculated as 29 pg/mL. Characteristic mass, m_0, for 4.0 mL sample solution introduced in 60 s was found as 114 pg. The summary of the analytical figures of merit investigated for the system is given Table 15.

Table 15 Analytical figures of merit for HG-AT-ETAAS system.

Limit of Detection, LOD, 3s/m (N=5) pg/mL	61
Limit of Quantification, LOQ, 10s/m (N=5) pg/mL	204
Characteristic Concentration, C_0 pg/mL	29
Characteristic Mass, m_0, pg	114

3.4 *In-situ* Trapping of SbH_3 on Ir coated W-coil (ETA)

W-coil was used as a trapping medium for SbH_3 as it was mentioned in section 3.2 to improve the sensitivity. The difference between these two trapping systems was the atomization units. W-coil mentioned in section 3.2 was employed as a trapping medium and after revolatilization species were sent to flame heated QTA for the atomization. In this manner W-coil was operating as an electrothermal vaporizer (ETV). In this part of the study W-coil was used as both atom trap and atomizer and thus its operation was named as electrothermal atomization (ETA).

In this systemi the gaseous SbH_3 was transported to a W-coil preheated to collection temperature and these species were collected for a certain period of time. When collection period was over, temperature of W-coil was increased rapidly to the atomization temperature and a transient signal was obtained.

Studies based on uncoated W-coil and Ir coated W-coil were carried out. It was observed that data obtained with uncoated W-coil were not reproducible. Surface modification of W-coil with Ir improved the sensitivity and results were reasonable. W-coil was coated with Ir according to the procedure given in section 2.6.5. A total mass of 250 µg of Ir was introduced to W-coil. Surface study was carried out by Scanning Electron Microscopy (SEM) in order to investigate the differences between uncoated W-coil, coated W-coil and W-coil used several times.

3.4.1 Argon Flow Rate

The optimum Ar flow rates at collection and atomization stages were determined and optimization graphs were given in Figure 29 and Figure 30, respectively. During these stages only Ar flow rate was varied for the determination of optimum gas flow rate for collection and atomization stages while H_2 flow rate was kept constant at 160 mL/min for both collection and atomization stages.

W-coil was easily oxidized in the presence of traces of O_2. Oxygen from air diffused through the open ends of the glass cell. Ar and H_2 flow rates should be sufficient to prevent the O_2 diffusion. Moreover, cooling effect of H_2 caused fluctuations in W-coil temperature during collection period at Ar flow rates lower than 400 mL/min; these sporadic changes were visible while W-coil was heated to glowing temperature. Therefore Ar flow rate should be high enough to prevent O_2 diffusion and keep temperature of W constant during collection stage. The temperature of W-coil was unstable and a background signal was observed when the Ar flow rate was 100 mL/min (Figure 28).

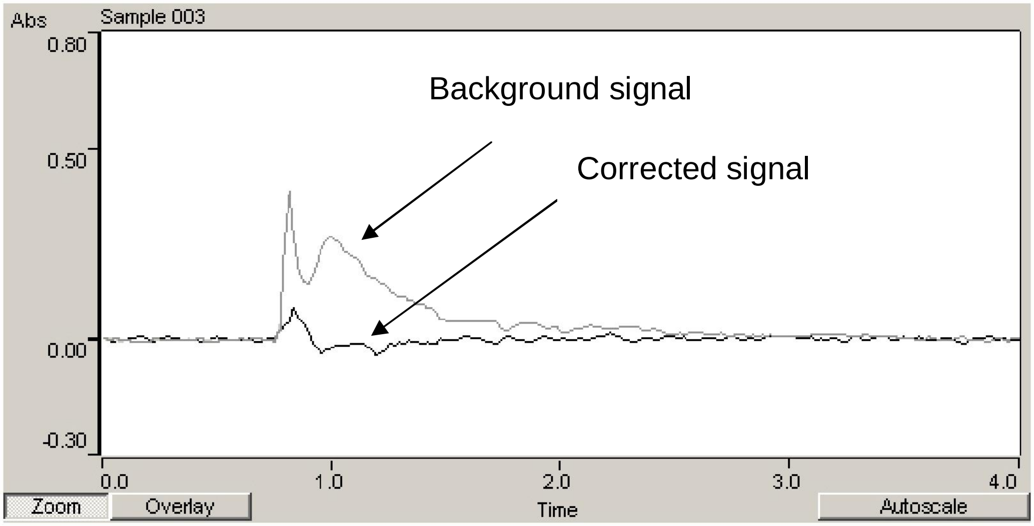

Figure 28 Effect of 100mL/min Ar flow rate at collection stage on W-coil-AT-HGAAS signal of 5.0 ng/mL Sb(III) solution trapped over 60 seconds time period. Sample solution was pumped at 4.0 mL/min. Trapping temperature and atomization temperatures were adjusted to 470 ºC and 2000 ºC, respectively.

As the Ar flow rate was increased background signal disappeared and temperature was kept constant. It was clear that the trapping efficiency increased at lower Ar flow rates. At high flow rates of Ar, transport of volatile species was achieved sufficiently at the collection stages; however high flow rates resulted in dilution of volatile species during collection stage. The optimum Ar flow rate at collection stages was chosen as 400 mL/min (Figure 29).

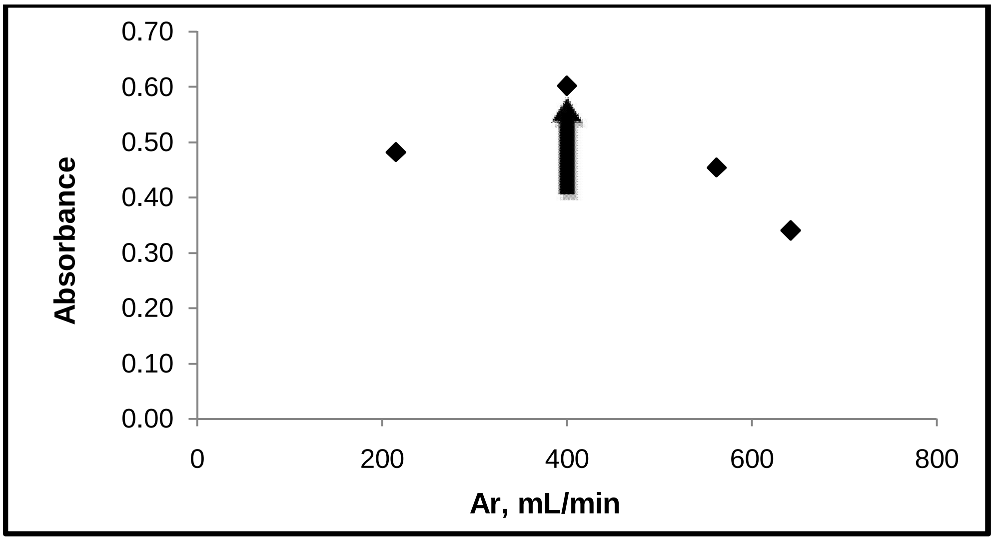

Figure 29 Effect of Ar flow rate at collection stage on W-coil-AT-HGAAS signal of 5.0 ng/mL Sb(III) solution trapped over 60 seconds time period. Sample solution was pumped at 4.0 mL/min. Trapping temperature and atomization temperatures were adjusted to 470 ºC and 2000 ºC, respectively.

For atomization stage, the optimum Ar flow rate was selected as 214 mL/min. The lower Ar flow rates for atomization stage caused a decrease in peak height. At high flow rates, the analytical signal became smaller due to the reduced residence time and dilution of analyte species in the atomizer. The effect of Ar flow rate at the atomization stage is given in Figure 30.

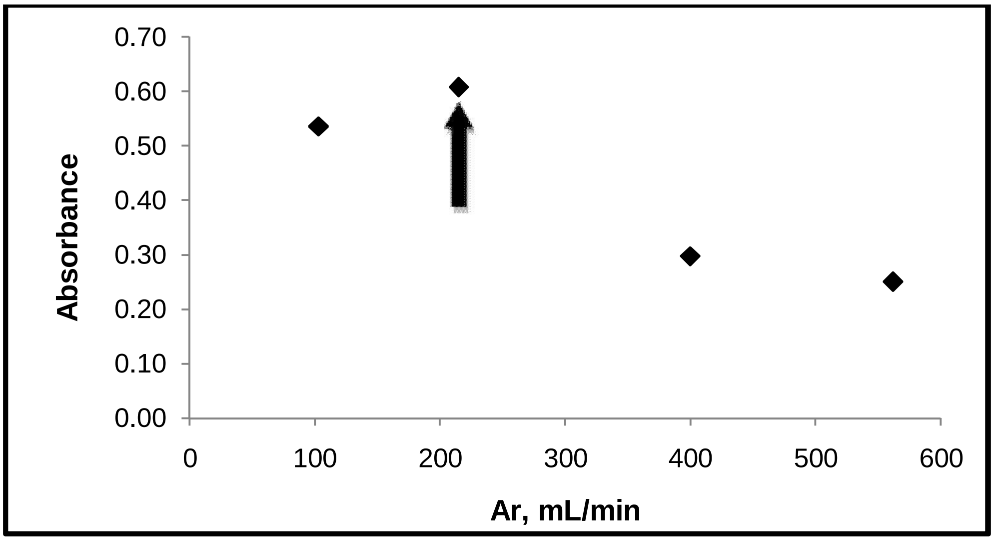

Figure 30 Effect of Ar flow rate at atomization stage on W-coil-AT-HGAAS signal of 5.0 ng/mL Sb(III) solution trapped over 60 seconds time period. Sample solution was pumped at 4.0 mL/min. Trapping temperature and atomization temperatures were adjusted to 470 ^oC and 2000 ^oC, respectively.

3.4.2 Hydrogen Flow Rate

In continuous flow HGAAS studies carrier gas was only Ar. However, W-coil was easily oxidized when it was heated in the presence of O_2; it was necessary to create a reducing environment in order to prevent oxidation. Although hydrogen was produced during HG process, this amount was insufficient to prevent the W-coil from being oxidized. Therefore additional H_2 gas was required to obtain a reducing environment and eliminate background signal resulted from oxidation.

The effect of H_2 on the collection efficiency was investigated by varying its flow rate during collection stage while keeping Ar flow rate constant. The plot of analytical signal versus H_2 flow rate is given in Figure 31. The decrease in analytical signal was considered to be the consequence of cooling effect of hydrogen since the flow rate of H_2 affected the temperature and temperature was critical for trapping stibine. At collection stage, flow rate of H_2 was chosen as 136 mL/min. Lower flow rates caused oxidation of W-coil.

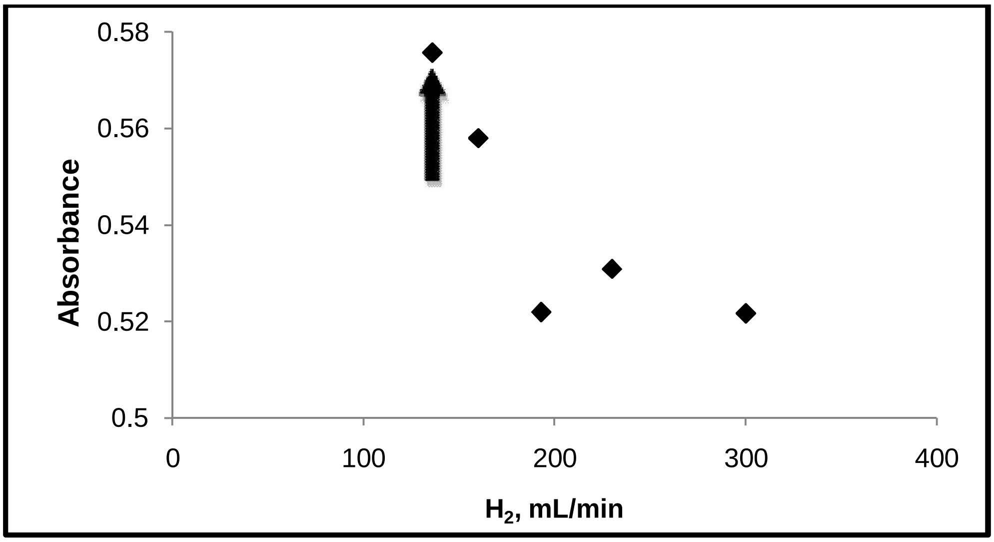

Figure 31 Effect of H_2 flow rate at collection stage on W-coil-AT-HGAAS signal of 5.0 ng/mL Sb(III) solution trapped over 60 seconds time period. Sample solution was pumped at 4.0 mL/min. Trapping temperature and atomization temperatures were adjusted to 470 ºC and 2000 ºC, respectively.

The effect of H_2 flow rate on analytical signal at atomization stage is given in Figure 32. The analytical signal did not change significantly with H_2 flow rate. The flow rate could not be decreased as for the collection stage since in this case the W-coil was oxidized and a background signal was observed. The optimum H_2 flow rate was selected as 136 mL/min. The same flow rate was used for collection and atomization stages since it was not practical to adjust gas flow rates at each cycle.

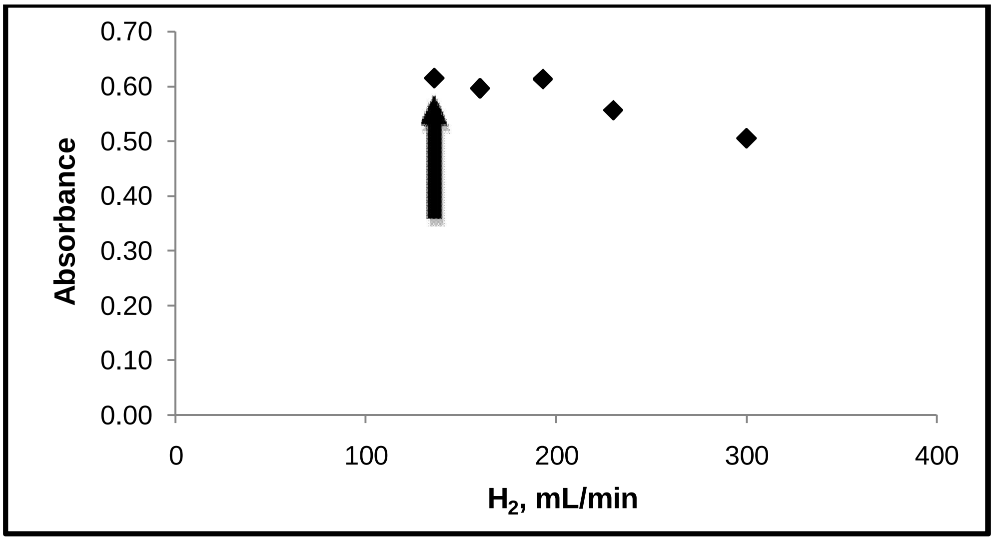

Figure 32 Effect of H_2 flow rate at atomization stage on W-coil-AT-HGAAS signal of 5.0 ng/mL Sb(III) solution trapped over 60 seconds time period. Sample solution was pumped at 4.0 mL/min. Trapping temperature and atomization temperatures were adjusted to 470 ºC and 2000 ºC, respectively.

3.4.3 Collection and Atomization Temperatures

The dependence of analytical signal on collection temperature is given in Figure 33. The optimum temperature at which maximum trapping was achieved by observing the signal obtained after each atomization cycle. The optimum collection temperature range was narrow and for temperatures higher than 500 ºC, a sharp decrease in signal due to loss of analyte by vaporization was observed. The optimum collection temperature for stibine was selected as 470 ºC.

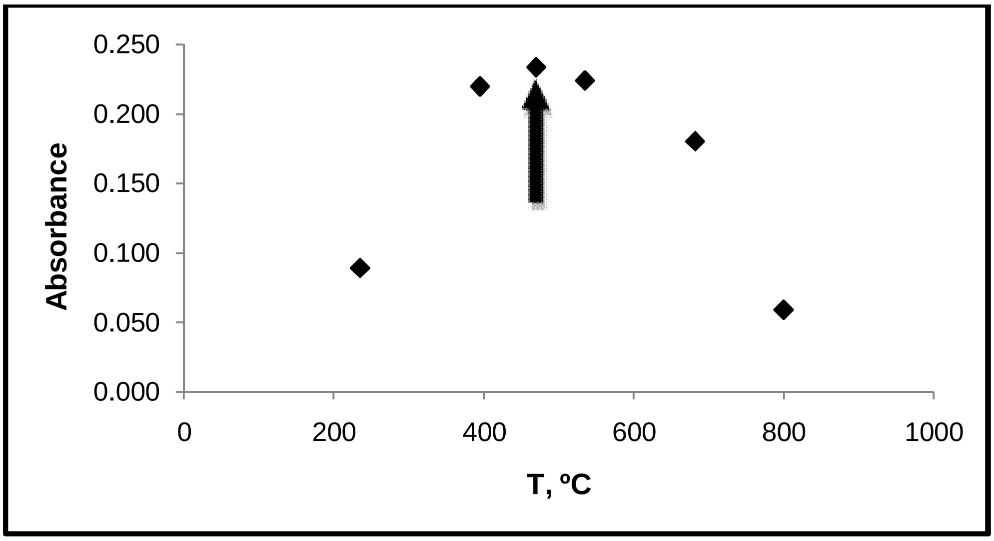

Figure 33 Effect of collection temperature on W-coil-AT-HGAAS signal of 5.0 ng/mL Sb(III) solution trapped over 60 second time period. Atomization temperature was kept at 2000 ºC.

In order to determine atomization temperature, the collection temperature was kept at 470 ºC and the atomization temperature was varied between 1465 ºC to 2200 ºC (Figure 34). The peak height of signal obtained at low temperature was low due to the slow rate of analyte release and thus broadening of the analytical signal was observed. As the temperature was increased, increase in analytical signal was observed and optimum atomization temperature was chosen as 2000 ºC. There was no significant change in the analytical signal for higher temperatures. At 2000 ºC analyte species could be released completely from W surface and therefore memory effect was not observed after atomization cycle.

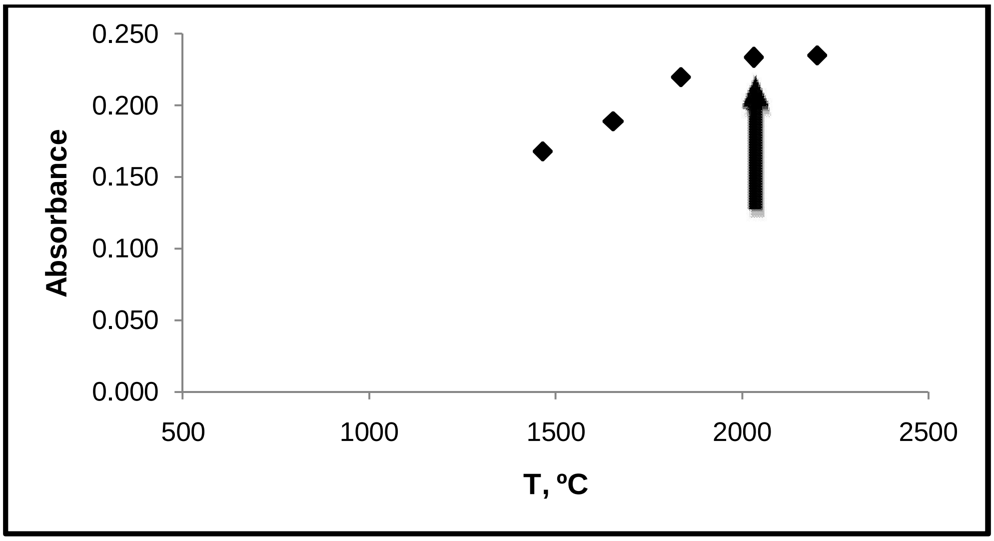

Figure 34 Effect of atomization temperature on W-coil-AT-HGAAS signal of 5.0 ng/mL Sb(III) solution trapped over 60 second time period. Collection temperature was kept at 470 ºC.

3.4.4 Collection Period

The relation between analytical signal and collection period was investigated by varying collection period between 30 seconds to 240 seconds and the results are displayed in Figure 35. The analytical signal increased linearly between the ranges of 30 seconds and 120 seconds. As the collection period increased, the signal did not further increase. 120 seconds was selected as the optimum collection period and calibration plot was obtained by using this value.

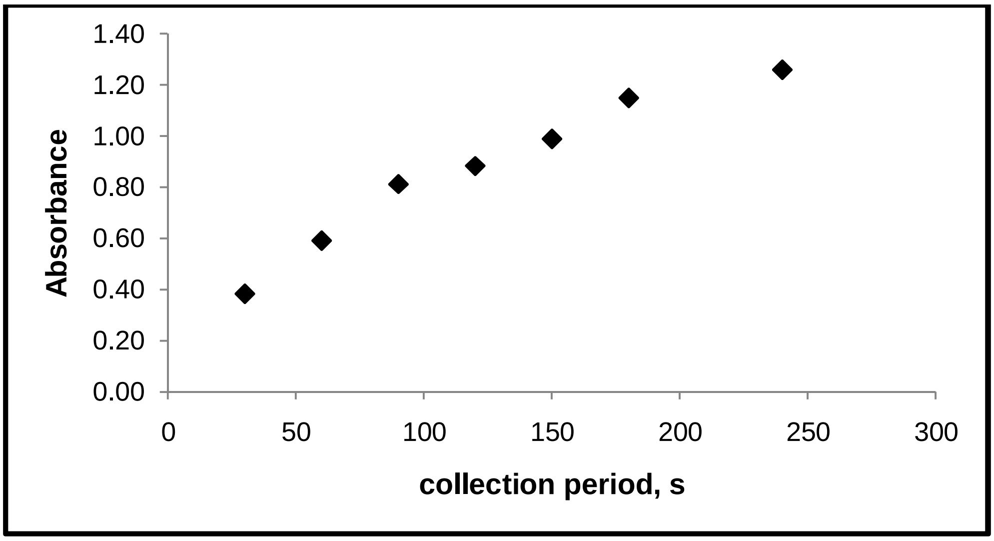

Figure 35 Effect of collection period on W-coil-AT-HGAAS signal of 5.0 ng/mL Sb solution pumped at 4.0 mL/min flow rate. Collection and atomization temperatures were adjusted to 470 ^{o}C and 2000 ^{o}C, respectively.

3.4.5 Calibration Plot and Linear Range

The calibration plot drawn by using a set of solution ranging from 0.5 ng/mL to 40.0 ng/mL Sb is given in Figure 36. The measurements were based on peak height of the analytical signal. It was found that the plot was linear between the concentrations of 0.5 ng/mL and 5.0 ng/mL Sb with a collection period of 120 seconds. Above this concentration deviation from linearity was observed. The best line equation and determination coefficient were, $y = 0.1307x + 0.0125$ and 0.9992, respectively (Figure 37).

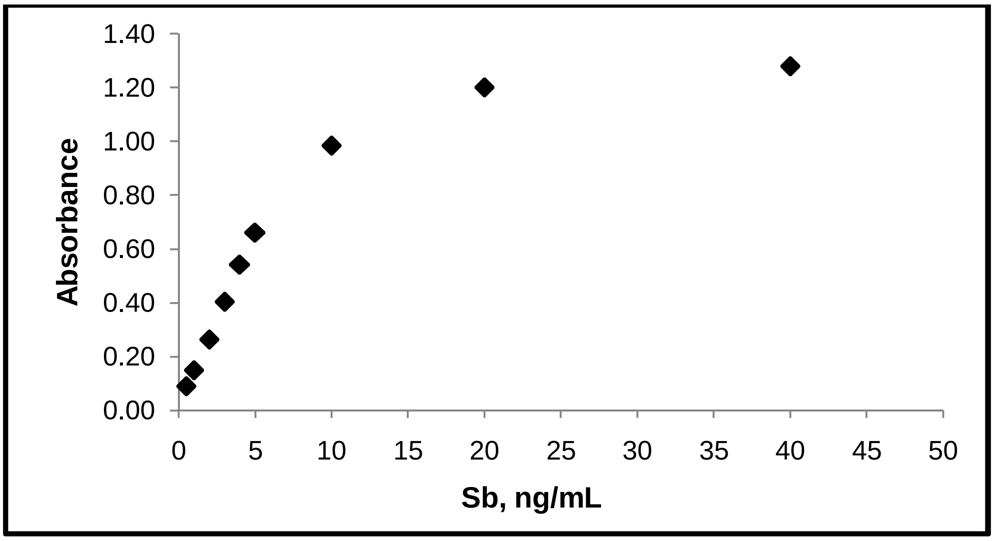

Figure 36 Calibration plot Sb using Ir coated W-coil-AT-HGAAS over 120 seconds collection period. Collection and atomization temperatures were 470 ºC and 2000 ºC, respectively. Sample flow rate was 4.0 mL/min.

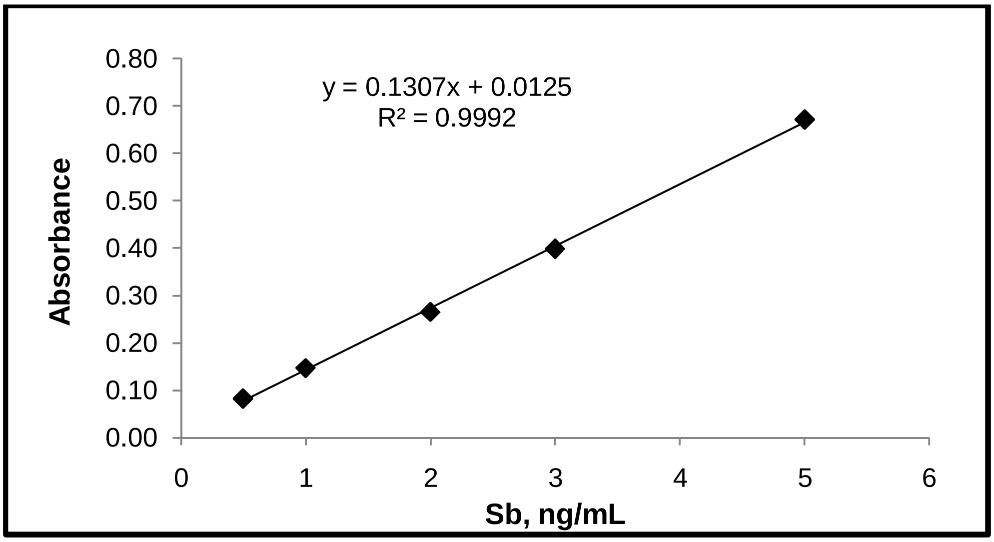

Figure 37 Linear portion of Ir coated W-coil-AT-HGAAS calibration plot and best line equation for Sb over 120 seconds collection period. Collection and atomization temperatures were 470 ºC and 2000 ºC, respectively. Sample flow rate was 4.0 mL/min.

3.4.6 Analytical Figures of Merit

LOD, LOQ, characteristic concentration, C_0, and characteristic mass, m_0, values for peak height were calculated as given in Table 16. Collection period was 120 seconds and 4.0 mL/min was used for both sample and $NaBH_4$ flow rates.

Table 16 Analytical figures of merit for Ir coated W-coil-AT-HGAAS.

Limit of Detection, LOD, pg/mL	152
Limit of Quantification, LOQ, pg/mL	508
Characteristic Concentration, C_0 pg/mL	33
Characteristic Mass, m_0, pg	263

The characteristic analytical signal for 5.0 ng/mL Sb(III) is given in Figure 38; the optimized conditions given in Table 17 were used. The half bandwidth of this signal was found to be 0.075 s.

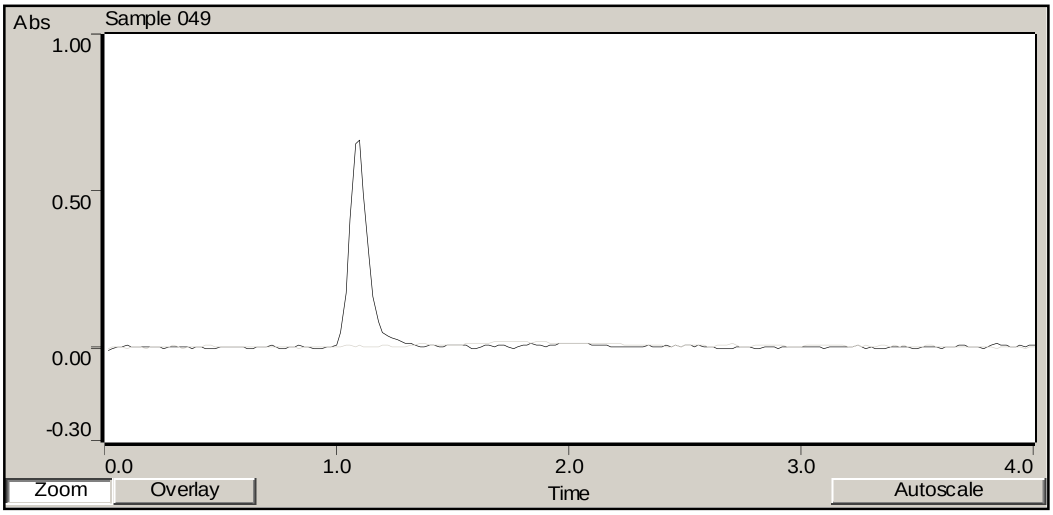

Figure 38 The signal of Ir coated W-coil-AT-HGAAS for 5.0 ng/mL Sb(III) trapped over 120 seconds. Conditions given in Table 17 were used.

The optimum conditions for Ir coated W-coil-AT-HG system are summarized in Table 17.

Table 17 Optimum Ir coated W-coil-AT-HG conditions.

PARAMETERS	RESULTS
Concentration of HCl, mol/L	0.050
Concentration of $NaBH_4$, % w/v	1.2
Flow rate of sample, mL/min	4.0
Flow rate of $NaBH_4$, mL/min	4.0
Length of reaction coil, cm	30.0
Length of stripping coil, cm	25.0
Collection Ar flow rate, mL/min	400
Atomization Ar flow rate, mL/min	214
Trapping H_2 flow rate, mL/min	136
Atomization H_2 flow rate, mL/min	136
Trapping temperature, ºC	470
Atomization temperature, ºC	2000

3.4.7 Accuracy Check

Accuracy of the method was tested by CRM, SCP SCIENCE, EnviroMAT-Waste Water, Low (EU-L-2). Before the analysis, reduction procedure described in section 2.6.6 was applied. Direct calibration method was used. Results were in good agreement with the certified values as shown in Table 18.

Table 18 Result of the Accuracy Test for Ir coated W-coil-AT-HGAAS using CRM, SCP SCIENCE, EnviroMAT-Waste Water, Low (EU-L-2).

	Certified Value	**Found Value**
Total Sb, ng/mL	18-20	18.1 ± 1.0

3.4.8 Speciation Studies

Inorganic Sb speciation was performed by Ir coated W-coil-AT-HGAAS system. Solutions containing different concentrations of Sb(III) and Sb(V) were prepared. The total content was kept constant at 5.0 ng/mL in the final solution and the reduction procedure given in section 2.6.6 was applied for total Sb determination.

These solutions were prereduced by 8.0% (w/v) KI and 0.10% (w/v) ascorbic acid and the absorbance value of total Sb was given in Figure 39. It could be seen from the plot that all Sb(V) species were reduced to Sb(III) by the reduction system applied.

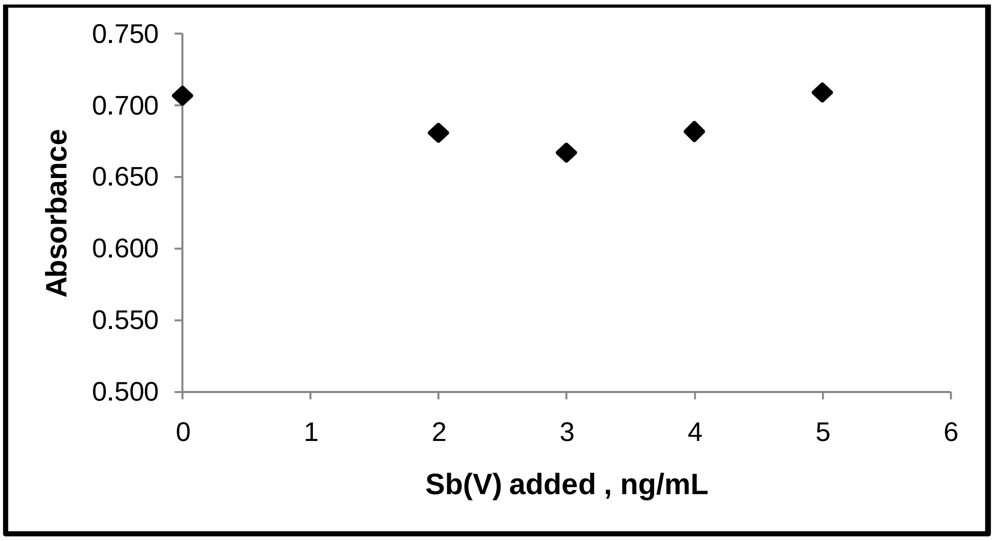

Figure 39 Absorbance values of mixtures after applying pre-reduction procedure by Ir coated W-coil-AT-HGAAS. Total concentration of Sb species was 5.0 ng/mL.

After the reduction process, total antimony species was determined. In order to obtain concenration of Sb(V) separately, difference of absorbance values of total Sb and Sb(III) was used. This difference was placed into the equation of calibration plot and concentration of Sb(V) could be found. Solutions containing totally 5.0 ng/mL Sb was used for the determination Sb(V). Spiked Sb(V) concentrations were compared with the found values (Table 19). It was observed that concentration of found Sb(V) was close to the concentration of spiked Sb(V). Additionally, it can be seen from Table 19 that recovery values of reduced Sb species were approximately 100%.

Table 19 Comparison of concentrations of spiked Sb(V) and found Sb(V).

Spiked Sb(V), ng/mL	Spiked Sb(III), ng/mL	Total Sb, ng/mL	Found Sb(V), ng/mL	Recovery, %
5.0	-	5.0	5.34±0.13	100.5
4.0	1.0	5.0	4.01±0.16	96.6
3.0	2.0	5.0	2.97±0.24	94.4
2.0	3.0	5.0	2.16±0.19	98.2
-	5.0	5.0	0.18±0.23	-

3.5 Evaluation of System Performance

Developed methods were compared in terms of sensitivity enhancement. In order to compare all the methods with each other direct liquid sampling ETAAS and W-coil-ETAAS were performed. The linear calibration plots for liquid sampling ETAAS and W-coil-ETAAS are given in Figure 40 and Figure 41, respectively.

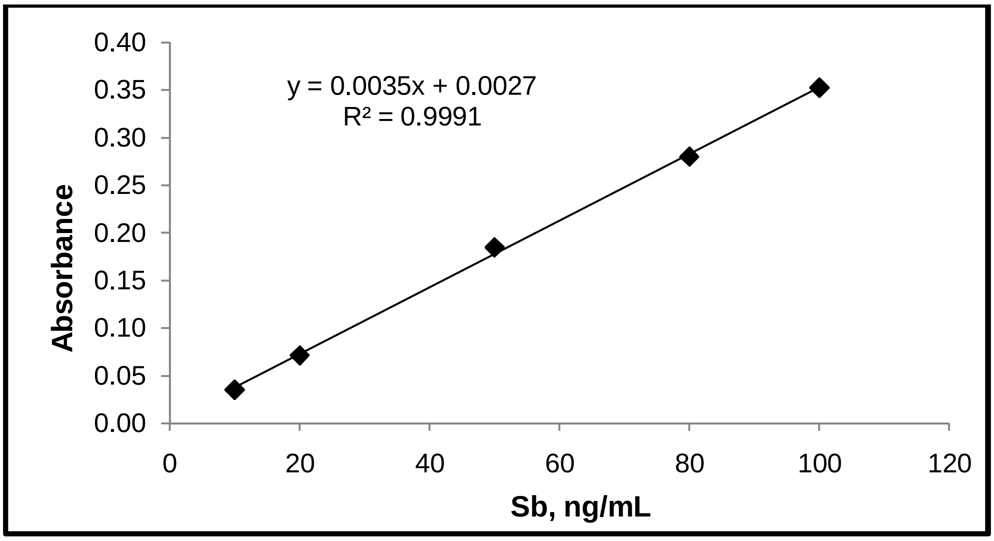

Figure 40 Linear calibration plot for Sb obtained by liquid sampling ETAAS. Sample volume was 15 µL.

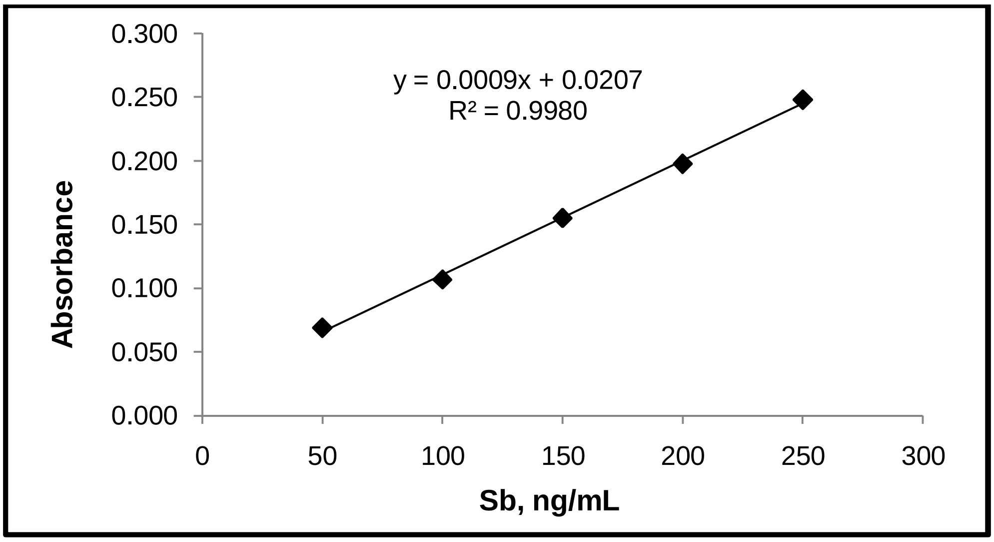

Figure 41 Linear calibration plot for Sb obtained by direct liquid sampling Ir coated W-coil-ETAAS. Sample volume was 20 µL.

LOD, LOQ, characteristic concentration (C_0) characteristic mass (m_0) values for peak height were calculated and given in Table 20 for both systems.

Table 20 Analytical figures of merit for direct liquid sampling ETAAS and W-coil-ETAAS.

	Liquid Sampling ETAAS	**Liquid Sampling W-coil-ETAAS**
Limit of Detection, LOD, ng/mL	2.4	21.3
Limit of Quantification, LOQ, ng/mL	8.1	71.1
Characteristic Concentration, C_0 ng/mL	1.2	4.2
Characteristic Mass, m_0, pg	18.0	84.0

Characteristic concentrations of developed methods are summarized in Table 21.

Table 21 Characteristic concentrations of developed methods.

	C_0, pg/mL
Liquid sampling W-coil-ETAAS	4200
Liquid sampling ETAAS	1200
CF-HGAAS	620
Ir coated W-coil-AT-HGAAS	33
HG-AT-HGAAS	29

Enhancement factor was calculated as the ratio of characteristic concentrations. However, sometimes enhancement factor become insufficient to compare sensitivity of methods since sample volume and/or time of integration changes from one method to the other. For this reason E_t, and E_v are the new terms used to normalize enhancement with respect to time and volume (Ataman, 2008). E_t, defined as enhancement factor for unit time and E_v, defined as enhancement factor for unit volume, have the units of min^{-1} and mL^{-1}, respectively. Enhancement factors, E_t and E_v values for developed methods Table 22 and Table 23.

Table 22 Comparison of the developed methods with respect to W-coil-ETAAS and CF-HGAAS.

	E with respect to liquid sampling W-coil-ETAAS	**E_t with respect to liquid sampling W-coil-ETAAS**	**E_v with respect to liquid sampling W-coil-ETAAS**	**E with respect to HGAAS**
Direct ETAAS	3.5			0.5
Continuous flow HGAAS	6.8			
Ir coated W-coil-AT-HGAAS, 8.0 mL sample collected in 2 min.	128	64	16	19
HG-AT-ETAAS, 4.0 mL sample collected in 1 min.	147	147	37	22

Table 23 Comparison of developed methods with respect to liquid sampling ETAAS.

	E with respect to liquid sampling ETAAS	E_t with respect liquid sampling to ETAAS	E_v with respect to liquid sampling ETAAS
Continuous flow HGAAS	1.9	-	-
Ir coated W-coil-AT-HGAAS, 8.0 mL sample collected in 2 min.	37	19	4.6
HG-AT-ETAAS, 4.0 mL sample collected in 1 min.	42	42	11

Ir coated W-coil-AT-HGAAS was compared with other methods developed for the determination of Sb (Table 24).

Table 24 Comparison of different methods used for determination of Sb regarding LOD and C_0 values.

	LOD, ng/mL	**C_0, ng/mL**	**Reference**
Quartz trap HGAAS, 8.0 mL sample collected in 120 s.	0.0039	-	Korkmaz, Dedina, & Ataman, 2004
Quartz trap EC-HGAAS, 6.0 mL sample collected in 120 s.	0.053	0.044	Menemenlioğlu, Korkmaz, & Ataman, 2007
Zr coated W-coil-EC-HGAAS, 20 mL sample collected in 5.0 min.	0.012	0.017	Yıldıran, 2008
HG-GFAAS with Pd modifier, 5.0 mL sample collected in 60 s.	0.014	-	Niedzielski & Siepak, 2003
Ir coated W-coil-AT-HGAAS, 8.0 mL collected in 120 s.	0.152	0.033	This study

3.6 Overall Efficiency

The overall efficiency of a HG system is based on the generation, transportation, trapping, revolatilization and atomization. It is difficult to determine efficiency of the system at each stage. The term overall efficiency is therefore used for the whole process. It can be estimated by *in-situ* trapping HG-AT-ETAAS using the signal from liquid sampling ETAAS. The sensitivity or characteristic mass of these techniques can be compared easily because sample introduction efficiency for liquid sampling is 100% and liquid matrix is removed in the vaporization and pyrolysis stages. Moreover, conditions in the atomization stage are nearly identical for both techniques **(Matousek, 2007)**.

In this study *in-situ* trapping HG-AT-ETAAS and liquid sampling ETAAS techniques were used to determine the overall efficiency of the system. Since the operations of W-coil-AT-HGAAS and liquid sampling W-coil-ETAAS techniques resemble to that of HG-AT-ETAAS and liquid sampling ETAAS, in turn, these techniques might be used so as to calculate overall efficiency. Overall efficiency values for HG-AT-ETAAS and W-coil-AT-HGAAS are given in Table 25.

Table 25 Overall efficiencies of HG-AT-ETAAS and W-coil-AT-HGAAS systems.

	Overall Efficiency, %
HG-AT-ETAAS	15
W-coil-AT-HGAAS	36

3.7 Interference Study

Interference study was performed for Ir coated W-coil-AT-HGAAS to determine the effect of other elements on Sb signal. Interfering elements were classified as hydride forming elements, cold vapor forming elements, transition metals and earth metals. Peak height values were taken into account to calculate the relative signal given in the following graphs. Sb solutions were prepared in 1 to 1, 1 to 10 and 1 to 100 mass ratios of analyte/interferent and concentration of Sb was kept constant at 3.0 ng/mL.

As, Se, Sn and Pb were selected as the group of hydride forming elements. The graphical representation of the interference effects of these elements on the absorbance signal are given in Figure 42. It can be seen from the graph that As did not have any significant effect on Sb signal. As the interferent concentration increased the interference effect of Se, Pb and Sn could be easily investigated. A pronounced effect of Sn was observed at 100 fold and it decreased peak height signal by 70%. The interference effects are believed to be taking place during hydride generation step. It has been stated that among the hydride forming elements the highest ranked interferent was Sn **(Dedina & Tsalev, 1995)**.

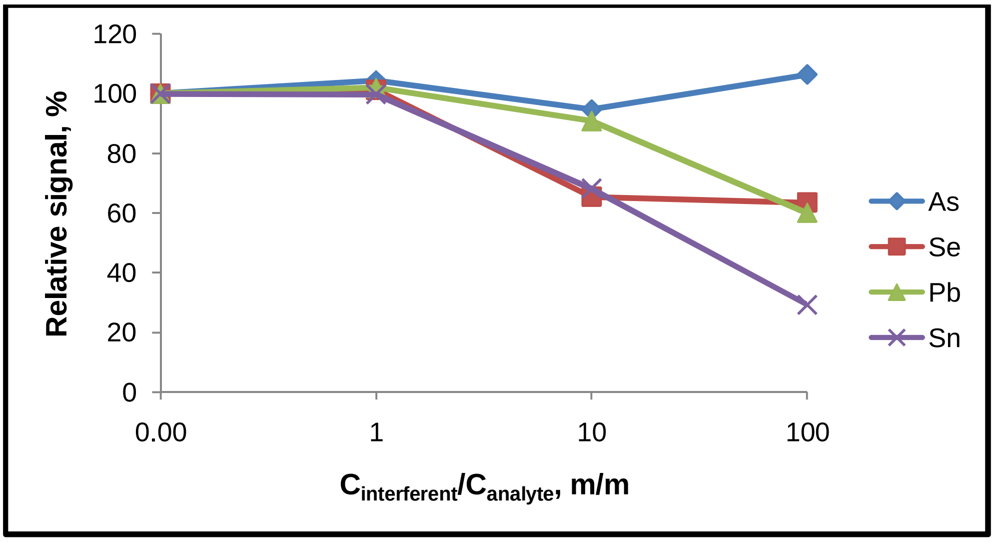

Figure 42 Effect of hydride forming elements on the W-coil-AT-HGAAS signal of 3.0 ng/mL Sb(III) solution trapped over 60 seconds.

To see the interference effect of transition metals, Fe, Co, Ni and Cu were selected for this group of elements. The effects of these elements on Sb signal are shown in Figure 43. Up to 100 fold excess the system was tolerable to the interference effects of Ni and Co, however at 100 fold Co and Ni reduced the Sb signal by 39% and 60%, respectively. Fe caused a decrease in Sb signal and signal was detoriated by around 40% for 100 fold. No significant interference was observed for Cu.

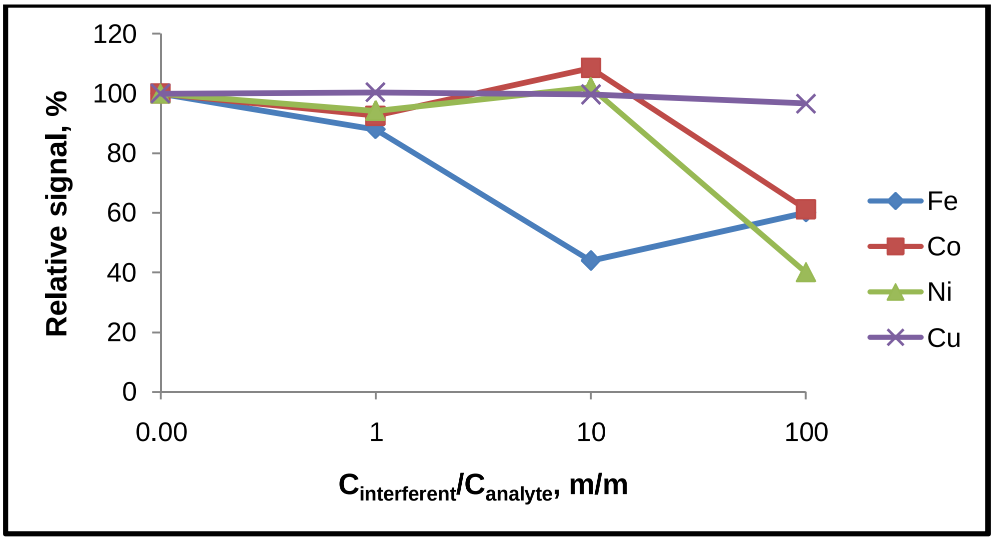

Figure 43 Effect of transition metals on the W-coil-AT-HGAAS signal of 3.0 ng/mL Sb(III) solution trapped over 60 seconds.

Hg and Cd were known as cold vapor forming elements. Interference effect of these elements was studied. Hg and Cd did not cause a significant suppression on the analytical signal and results are given in Figure 44. Relative high volatility of these elements may be the result of this situation.

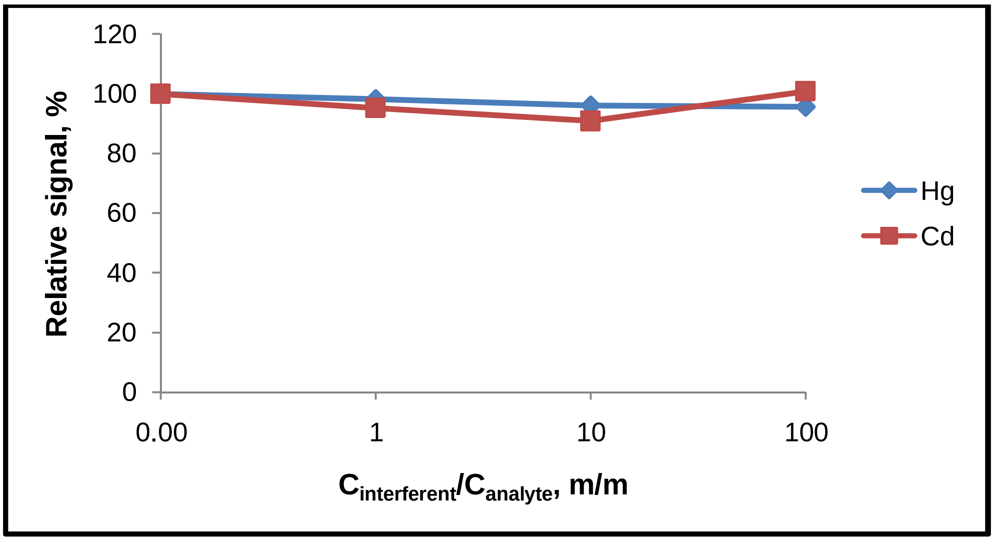

Figure 44 Effect of cold vapor forming elements on the W-coil-AT-HGAAS signal of 3.0 ng/mL Sb(III) solution trapped over 60 seconds.

Finally the interference effect of soil based elements was studied. Al and Ca were selected as the representative elements for the study. Effects of these elements on the analytical signal are represented in Figure 45. Al suppressed the signal by 21% at 100 fold and had no effect on analytical signal on the other ratios. The decrease in signal was observed Ca. The suppression effect of Ca was 28 and 36% at mass ratios of 10 and 100, respectively. After 60 second trapping, the release of Ca from W-coil was difficult. Ca was removed from surface after applying 2 or 3 times firing.

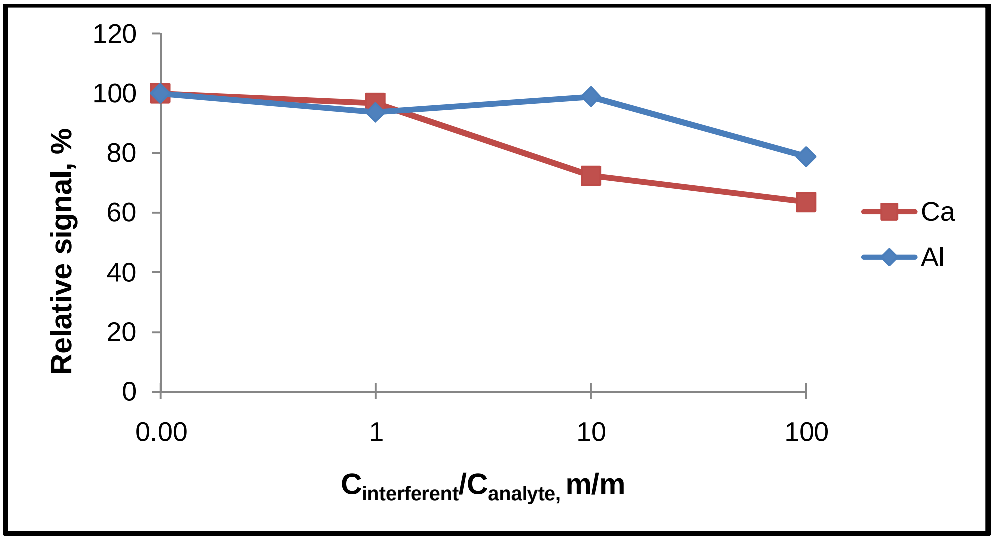

Figure 45 Effect of Ca and Al elements on the W-coil-AT-HGAAS signal of 3.0 ng/mL Sb(III) solution trapped over 60 seconds.

3.8 Surface Study

Surface of different W-coils were investigated with SEM. Variation on the surface depending on the use was observed. For this purpose SEM images of uncoated and unused W-coil, unused Ir coated W-coil and finally Ir coated W-coil that was used several times were taken. The differences between surfaces were apparent. The image of uncoated and unused W-coil is given in Figure 46.

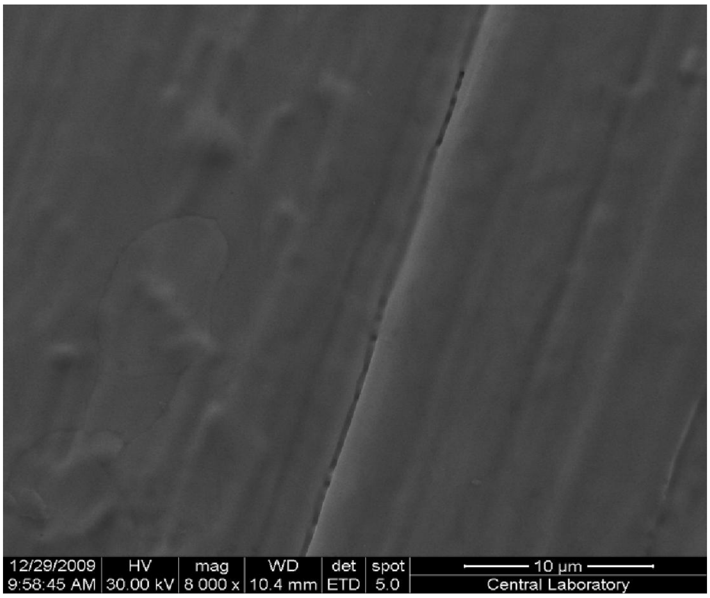

Figure 46 SEM image of unused and uncoated W-coil in the scale of 10 µm.

The surface of Ir coated and unused W-coil was examined and image of coil is shown in Figure 47. As can be seen from Figure 46 and Figure 47, there was a distinct difference between the surfaces of W-coils. Ir coated W-coil was used for several times and SEM image of this coil was then taken. Its image is given in Figure 48.

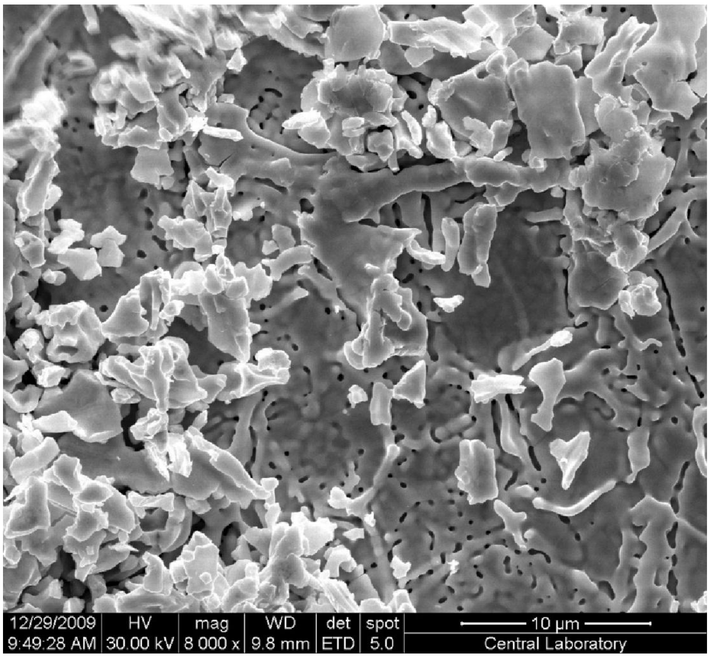

Figure 47 SEM image of unused Ir coated W-coil in the scale of 10 µm.

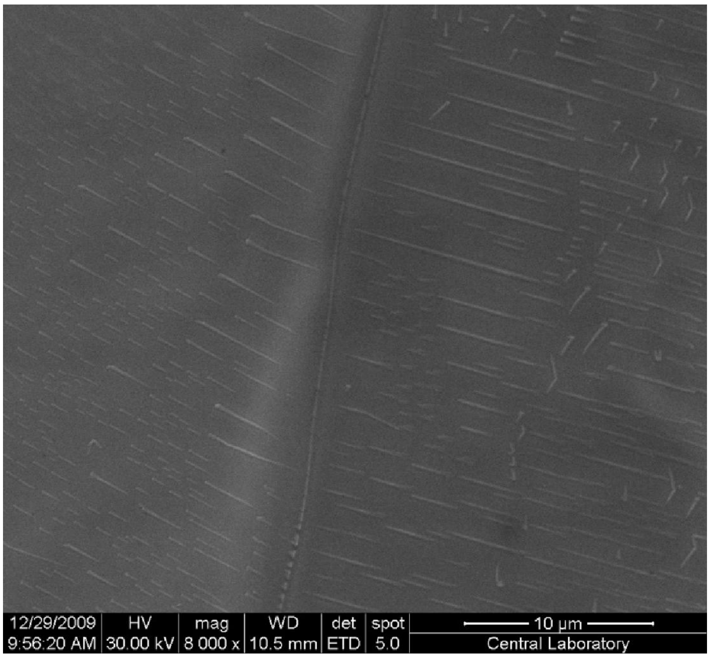

Figure 48 SEM image of Ir coated W-coil after approximately 150 firings in the scale of 10 µm.

CHAPTER 4

CONCLUSIONS

The aim of this study was to develop a sensitive and simple method for the determination and inorganic speciation of Sb.

In the first part of study, hydride generation conditions were optimized with CF-HGAAS. Moreover, speciation study was performed with CF-HGAAS system and optimum reduction conditions were determined. Reduction of Sb(V) species to Sb(III) species was achieved by 8.0% (w/v) KI and 0.10% (w/v) ascorbic acid. Recoveries of solution with different contents of Sb(V) and Sb(III) were around 100%.

Second part of the study includes attempts to develop a method for Sb determination with HG-W-coil-ETV. W-coil was used as a trapping medium and a vaporizer unit. The atomizer was a flame heated QTA. Some challenges were faced during the study. First of all, at the collection stage, the quartz surface was heated sufficiently to trap some of the Sb species. Two subsequent signals were observed after revolatilization stage. The second one was thought to be belonging to released species from quartz surface. Secondly, there were problems related with the temperature applied at revolatilization stage. Since high temperature was used for the release of trapped analyte species from W-coil, surface of the coil was deformed. W species evolved from the coil accumulated on the quartz surface and a new trapping medium took place. Analytical signal of the last firing was 50% less than that of first signal. While the studies concerning HG-W-coil-ETV were proceeding HG-AT-ETAAS study was performed to investigate whether there was a problem regarding hydride generation system.

The third part of the study deals with the search on *in-situ* trapping of SbH_3 on graphite tube. The hydride generation conditions optimized in continuous flow HGAAS system were used except that the stripping Ar flow. Ar flow rate had a critical role on the analytical signal of Sb. It was found that stripping Ar flow rate was lower in HG-AT-ETAAS than in CF-HGAAS as it was expected. The low flow rate caused inefficient transport of SbH_3 to the graphite furnace and high flow rate resulted in the dilution of analyte atoms during atomization stage. Ar flow rate of 100 mL/min was used during this part of the study. Collection and atomization temperatures were set to 750 ºC and 2000 ºC, respectively. LOD and LOQ value of the system was 61 pg/mL and 204 pg/mL, respectively. The enhancement factor with respect to ETAAS was 42. Moreover, HG-AT-ETAAS and liquid sampling ETAAS were used to calculate the overall efficiency of the HG sysyem.

The fourth part of the study involves the development of a sensitive method that is *in-situ* trapping of SbH_3 on Ir coated W-coil, namely Ir coated W-coil-AT-HGAAS. W-coil was used as a trapping medium and an atomizer. Ir was used as a permanent modifier and total mass of 250 µg Ir (1000 mg/L) was used for coating of W-coil. Coating was stable up to around 300 firings. When loss of sensitivity was observed W-coil was recoated with Ir. The Ar flow rate had a significant role on temperature control during collection stage. Low Ar flow rates resulted in the instability of temperature and oxidation of W-coil. High flow rates caused decrease of analytical signal due to the dilution and 400 mL/min was selected as the optimum value during the collection stage. At atomization stage Ar was required for the release of analyte from W-coil and 214 mL/min was chosen as the optimum value at atomization stage. H_2 gas was required to form a reducing environment in order to prevent oxidation of W-coil. Optimum value for the H_2 flow rate was selected as 136 mL/min for both collection and atomization stage. Collection and atomization temperatures were 470 ºC and 2000 ºC, respectively. For the developed method LOD and LOQ values were found as 152 pg/mL and 508 pg/mL, respectively. 128 and 37 fold enhancements were obtained with respect to W-coil-ETAAS and ETAAS. The accuracy of the method was tested by the use of CRM that is SCP SCIENCE EnviroMAT Low (EU-L 2). The results were in good agreement with the certified value.

Interference study was performed for Ir coated W-coil-AT-HGAAS system. The effect of soil based elements, some hydride forming elements and some transition metals on the analytical signal of Sb were investigated. Among hydride forming elements Sn suppressed the signal significantly. Moreover, Fe and Ni affect the signal at high concentrations.

Lastly, surface study was performed to investigate the differences between different W-coil surfaces. For this aim, uncoated and unused W-coil, Ir coated and unused W-coil and lastly Ir coated W-coil used several times were used for the surface study. The SEM images were taken for all kinds of W-coil. Distinct differences regarding their surface morphology were observed.

Inorganic speciation of Sb study was performed using Ir coated W-coil-AT-HGAAS. It has been demonstrated that inorganic speciation with this system is feasible. Both oxidation states of Sb could be determined selectively by this developed method. However, speciation of inorganic Sb could not be performed with EC-HGAAS system. Since hydrides of both of the oxidation states were generated and trapped with the same efficiency with Zr coated W-coil-EC-HGAAS, this method allows total inorganic Sb determination **(Yıldıran, 2008)**.

To conclude, Ir coated W-coil-AT-HGAAS is a sensitive analytical method for the determination of antimony. In this study, W-coil was used as both an atom trap and atomization unit. According to the results it can be concluded that there is not so much difference between W-coil-AT-HGAAS and HG-AT-

ETAAS regarding the sensitivity. The other important point for the comparison of two techniques is their cost. W-coil is easily available and more economical compared to a graphite cuvette.

REFERENCES

A, D., C, B., E, P., M, O., & R, Z. (2004). Chemical vapor generation for atomic spectrometry. A contribution to the comprehension of reaction mechanisms in the generation of volatile hydrides using borane complexes. *Spectrochim. Acta, Part B , 59*, 471-486.

Ali, I., & Aboul-Enein, H. Y. (2006). *Instrumental Metal Ion Speciation.* Baco Raton: CRC/TaylorFrancis.

Alp, O., & Ertaş, N. (2008). In-situ trapping of antimony hydride on iridium-coated tungsten coil and interference studies. *J. Anal. At. Spectrom. , 23*, 976-980.

Andreae, M. 0., Asmodi, J. F., Foster, P., & Dack, L. V. (1981). Determination of Antimony(III), Antimony(V), and Methylantimony Species in Natural Waters by Atomic Absorption Spectrometry with Hydride Generation. *Anal. Chem. , 53*, 1766-1771.

Ataman, O. Y. (2008). Vapor generation and atom traps: Atomic absorption spectrometry at the ng/L level. *Spectrochim. Acta, Part B , 63*, 825–834.

Barbosa, F., Souza, S. S., & Krug, F. J. (2002). In situ trapping of selenium hydride in rhodium-coated tungsten coil electrothermal atomic absorption spectrometry. *J. Anal. At. Spectrom. , 17*, 382-388.

Berndt, H., & Schaldach, G. (1988). Simple Low Cost Tungsten Coil Atomizer For Electrothermal Atomic Absorption Spectrometry. *J. Anal. Atom. Spectrom. , 3*, 709-712.

Broekaert, J. A. (2005). *Analytical Atomic Spectrometry with Flames and Plasmas.* Germany: WILEY-VCH.

Cankur, O., Ertas, N., & Ataman, O. Y. (2002). Determination of bismuth using on-line preconcentration by trapping. *J. Anal. At. Spectrom. , 17*, 603–609.

Chen, B., Krachler, M., & Shotyk, W. (2003). Determination of antimony in plant and peat samples by hydride generation-atomic fluorescence spectrometry (HG-AFS). *J. Anal. At. Spectrom. , 18*, 1256-1262.

Chu, R. C., Barron, G. P., & Baumgarner, P. A. (1972). Arsenic Determination at Sub Microgram Levels by Arsine Evolution and Flameless Atomic Absorption Spectrophotometric Technique. *Anal. Chem. , 44*, 1476-1479.

Council of the European Communities. (1998). *Council Directive Relating to the Quality of Water Intented Human Consumption , 98/83/CE* .

Dedina, J., & Rubeska, I. (1980). Hydride atomization in a cool hydrogen–oxygen flame burning in a quartz tube atomizer. *Spectrochim. Acta, Part B , 35*, 119–128.

Dedina, J., & Tsalev, D. L. (1995). *Hydride Generation Atomic Absorption Spectrometry.* Chichester: John Wiley and Sons Ltd.

Dedina, J., & Matousek, T. (2000). Multiple microflame—a new approach to hydride atomization for atomic absorption spectrometry. *J. Anal. At. Spectrom. , 15*, 301 - 304.

Dedina, J. (2007). Atomization of volatile compounds for atomic absorption and atomic fluorescence spectrometry: On the way towards the ideal atomizer. *Spectrochim. Acta, Part B , 62*, 846–872.

Docekal, B., Güçer, Ş., & Selecka, A. (2004). Trapping of hydride forming elements within miniature electrothermal devices: part 1. Investigation of collection of arsenic and selenium hydrides on a molybdenum foil strip. *Spectrochim. Acta, Part B , 59*, 487-495.

Drasch, G., Meyer, L. V., & Kauert, G. (1980). Application of the furnace AA method for the detection of As in biological samples by means of hydride technique. *Fresenius J. Anal. Chem. , 304*, 141-142.

D’Ulivo, A., Baiocchi, C., Pitzalis, E., Onor, M., & Zamboni, R. (2004). Chemical vapor generation for atomic spectrometry. A contribution to the comprehension of reaction mechanisms in the generation of volatile hydrides using borane complexes. *Spectrochim. Acta, Part B , 59*, 471-486.

D'Ulivo, A., Mester, Z., & Sturgeon, R. (2005). The mechanism of formation of volatile hydrides by tetrahydroborate(III) derivatization: a mass spectrometric study performed with deuterium labelled reagents. *Spectrochim. Acta, Part B , 60*, 423–438.

D'Ulivo, A., Mester, Z., Meija, J., & Sturgeon, R. E. (2006). Gas chromatography–mass spectrometry study of hydrogen–deuterium exchange reactions of volatile hydrides of As, Sb, Bi, Ge and Sn in aqueous media. *Spectrochim. Acta, Part B , 61*, 778-787.

Erdem, A., & Eroğlu, A. E. (2005). Speciation and preconcentration of inorganic antimony in waters by Duolite GT-73 microcolumn and determination by segmented flow injection-hydride generation atomic absorption spectrometry (SFI-HGAAS). *Talanta , 68*, 86-92.

Filella, M., Belzile, N., & Chen, Y. W. (2002). Antimony in the environment: A review focused on natural waters I. Occurrence. *Earth-Sci. Rev. , 57*, 124-176.

Filella, M., Belzile, N., & Chen, Y. W. (2002). Antimony in the environment: A review focused on natural waters II. Relevant solution chemistry. *Earth-Sci Rev. , 59*, 265-285.

Filella, M., Belzile, N., & Lett, M. C. (2007). Antimony in the environment: A review focused on natural waters. III. Microbiota relevant interactions. *Earth-Sci. Rev. , 80*, 195-217.

Garcia, I. L., Merlos, M. S., & Cordoba, M. H. (1997). Arsenic and antimony determination in soils and sediments by graphite furnace atomic absorption spectrometry with slurry sampling. *Spectrochim. Acta, Part B , 52*, 437-443.

Guo, X. M., & Guo, X. W. (2001). Determination of ultra-trace amounts of selenium by continuous flow hydride generation AFS and AAS with collection on gold wire. *J. Anal. At. Spectrom. , 16*, 1414-1418.

Holak, W. (1969). Gas-sampling technique for arsenic determination by atomic absorption spectrophotometry. *Anal. Chem. , 41*, 1712-1713.

International Agency for Research on Cancer (IARC). (1989). *47* , 291.

İsmail, O. (2000). Determination of cadmium by cold vapor generation atom trapping atomic absorption spectrometry. *M.S thesis* . Ankara, Turkey: Middle East Technical University.

Kentner, M., Leinemann, M., Schaller, K. H., Weltle, D., & Lehnert, G. (1995). External and internal antimony exposure in starter battery production. *Int. Arch. Occup. Environ. Health , 67*, 119.

Korkmaz, D. K., Ertaş, N., & Ataman, O. Y. (2002). A novel silica trap for lead determination by hydride generation atomic absorption spectrometry. *Spectrochim Acta, Part B* (57), 571-580.

Korkmaz, D., Dedina, J., & Ataman, O. Y. (2004). Stibine preconcentration in a quartz trap with subsequent atomization in the quartz multiatomizer for atomic absorption spectrometry. *J. Anal. At. Spectrom. , 19*, 255-259.

Kratzer, J., & Dedina, J. (2008). Stibine and bismuthine trapping in quartz tube atomizers for atomic absorption spectrometry — Method optimization and analytical applications. *Spectrochim. Acta, Part B , 63*, 843-849.

Krupp, E. M., Grumping, R., Furchtbar, U. R., & Hirner, A. V. (1996). Speciation of metals and metalloids in sediments with LTGC/ICP-MS. *Fresenius J. Anal. Chem. , 354*, 546-549.

Kubota, T., Kawakami, A., Sagara, T., Ookubo, N., & Okutani, T. (2001). Determination of antimony content in natural waters by graphite furnace atomic absorption spectrometry after collection as antimony(III)-pyrogallol complex on activated carbon. *Talanta , 53*, 1117-1126.

Kula, İ., Arslan, Y., Bakırdere, S., & Ataman, O. (2008). A novel analytical system involving hydride generation and gold-coated W-coil trapping atomic absorption spectrometry for selenium determination at ng l−1 level. *Spectrochim. Acta, Part B , 63*, 856–860.

Kumar, A. R., & Riyazuddin, P. (2007). Non-chromatographic hydride generation atomic spectrometric techniques for the speciation analysis of arsenic, antimony, selenium, and tellurium in water samples—a review. *Int. J. Environ. Anal. Chem. , 87*, 469–500.

Matousek, T. (2007). The efficiency of chemical vapour generation of transition and nobel metals. *Anal. Bioanal. Chem. , 388*, 763-767.

Matusiewicz, H., & Krawczyk, M. (2008). Determination of total antimony and inorganic antimony species by hydride generation situ trapping flame atomic absorption spectrometry: a new way to (ultra)trace speciation. *J. Anal. At. Spectrom. , 23*, 43–53.

Menegario, A. A., Smichowsk, P., Tonello, P. S., Polla, G., Oliveira, E. P., & Santelli, R. E. (2008). On-line redox speciation analysis of antimony using l-proline immobilized on controlled pore glass and hydride generation inductively coupled plasma optical emission spectrometry for detection. *Anal. Chim. Acta , 625*, 131-136.

Menemenlioğlu, İ., Korkmaz, D., & Ataman, O. Y. (2007). Determination of antimony by using a quartz atom trap and electrochemical hydride generation atomic absorption spectrometry. *Spectrochim. Acta, Part B , 62*, 40-47.

Miekeley, N., Mortari, S. R., & Schubach, A. O. (2002). Monitoring of total antimony and its species by ICP-MS and on-line ion chromatography in biological samples from patients treated for leishmaniasis. *Anal. Bioanal.Chem. , 372*, 495-502.

Miravet, R., López-Sánchez, J. F., & Rubio, R. (2004). Comparison of pre-reducing agents for antimony determination by hydride generation atomic fluorescence spectrometry. *Anal. Chim. Acta , 511*, 295-302.

Niedzielski, P., & Siepak, M. (2003). Determination of Sb(III) and Sb(V) in Water Samples by Hydride Generation Atomic Absorption Spectrometry with In-Situ Trapping in a Graphite Tube. *Anal. Lett. , 36* (5), 971–986.

Pacheco, P. H., Gil, R. A., Martinez, L. D., Polla, G., & Smichowski, P. (2007). A fully automated system for inorganic antimony preconcentration and speciation in urine. *Anal. Chim. Acta , 603*, 1-7.

Quiroz, W., Gregori, I. D., Basillo, P., Pinto, M., & Lobos, M. G. (2009). Heavy weight vehicle traffic and its relationship with antimony content in human blood. *J. Environ. Monit. , 11*, 1051-1055.

Ribeiro, A. S., Arruda, M. A., & Cadore, S. (2002). A quartz tube atomizer with tungsten coil: a new system for vapor atomization in atomic absorption spectrometry. *J. Anal. At. Spectrom. , 17*, 1516-1522.

Rigin, V. L. (1978). Dispersionless AF Determination of As in Biological Materials. *J. Anal. Chem. USSR-Engl. Tr , 33*, 1966.

Robbins, W. B., & Caruso, J. A. (1979). Development of hydride generation methods for atomic spectroscopic analysis. *Anal. Chem. , 51*, 889-899.

Siemer, D. D., & Hageman, L. (1975). An improved HG AA apparatus for Se determination. *Anal. Lett. , 8*, 323-337.

Smichowski, P. (2008). Antimony in the environment as a global pollutant: A review on analytical methodologies for its determination in atmospheric aerosols. *Talanta , 75*, 2-14.

Smichowski, P., & Farias, S. (2000). Advantages and analytical applications of chloride generation. A review on vapor generation methods in atomic spectrometry. *Microchem.l J. , 67*, 147-155.

Sturgeon, R. E., Willie, S. N., Sproule, G. I., Robinson, P. T., & Berman, S. S. (1989). Sequestration of volatile element hydrides by platinum group elements graphite furnace atomic absorption. *Spectrochim. Acta, Part B , 44*, 667-682.

Thompson, K. C., & Thomerson. (1974). AA studies on the determination of sb, As, Bi, Ge, Pb, Se, Te and Sn by utilizing the generation of covalent hydrides. *Analyst , 99*, 595-601.

USEPA Drinking Water Contaminants. (2009). Retrieved 2009, from U.S Environmental Protection Agency: http://www.epa.gov/safewater/contaminants/index.html#inorganic

Welz, B., & Sperling, M. (1999). *Atomic Absorption Spectrometry.* Weinheim, Germany: WILEY-VCH.

Williams, M., & Piepmeier, E. H. (1972). Commercial Tungsten Filament Atomizer For Analytical Atomic Spectometry. *Anal. Chem. , 44*, 1342-1344.

Yıldıran, A. (2008). Electrochemical hydride generation and tungsten atom trap atomic absorption spectrometry for determination of antimony. *M.S Thesis* . Ankara, Turkey: Middle East Technical University.